The Plant Cell, Vol. 32: 486–507, February 2020, www.plantcell.org © 2020 ASPB.

A Tripartite Interaction among the Basidiomycete *Rhodotorula mucilaginosa*, N_2-Fixing Endobacteria, and Rice Improves Plant Nitrogen Nutrition

Karnelia Paul,[a,1] Chinmay Saha,[a,b,1,2] Mayurakshi Nag,[a] Drishti Mandal,[c] Haraprasad Naiya,[a,d] Diya Sen,[e,f] Souvik Mitra,[g] Mohit Kumar,[h] Dipayan Bose,[i] Gairik Mukherjee,[a] Nabanita Naskar,[j,k] Susanta Lahiri,[j] Upal Das Ghosh,[l] Sudipta Tripathi,[m] Mousumi Poddar Sarkar,[n] Manidipa Banerjee,[h] Aleysia Kleinert,[o] Alexander J. Valentine,[o] Sucheta Tripathy,[f] Senjuti Sinharoy,[c] and Anindita Seal[a,3]

[a] Department of Biotechnology and Dr. B.C. Guha Centre for Genetic Engineering and Biotechnology, University of Calcutta, Kolkata 700019, India
[b] Department of Endocrinology & Metabolism, Institute of Post Graduate Medical Education & Research and SSKM Hospital, Kolkata 700020, West Bengal, India
[c] National Institute of Plant Genome Research, New Delhi 110067, India
[d] ICAR-Indian Institute of Natural Resins and Gums Namkum, Ranchi 834010, Jharkhand, India
[e] Department of Plant Protection Biology, Swedish University of Agricultural Sciences, Stockholm, SE 75007, Sweden
[f] Computational Genomics Laboratory, Structural Biology and Bioinformatics Division, Council of Scientific and Industrial Research-Indian Institute of Chemical Biology, Kolkata 700032, India
[g] Department of Botany, Darjeeling Government College, Darjeeling 734101, India
[h] Kusuma School of Biological Sciences, Indian Institute of Technology Delhi, New Delhi 110016, India
[i] Crystallography and Molecular Biology Division, Saha Institute of Nuclear Physics, Kolkata 700064, India
[j] Saha Institute of Nuclear Physics, Kolkata 700064, India
[k] Department of Environmental Science, University of Calcutta, Kolkata 700019, India
[l] P.G. Department of Botany, Bidhannagar College, Kolkata 700026, India
[m] Agricultural Experimental Farm, Institute of Agricultural Science, University of Calcutta, Kolkata 700144, India
[n] Department of Botany, University of Calcutta, Kolkata 700019, India
[o] Botany & Zoology Department, University of Stellenbosch Private Bag X1 Matieland 7602 South Africa

ORCID IDs: 0000-0002-3921-7800 (K.P.); 0000-0002-6983-9336 (C.S.); 0000-0001-6291-4586 (M.N.); 0000-0002-1463-8596 (D.M.); 0000-0001-9260-719X (H.N.); 0000-0001-8097-7310 (D.S.); 0000-0003-3526-9942 (S.M.); 0000-0003-3147-3161 (M.K.); 0000-0001-9863-5538 (D.B.); 0000-0002-6181-891X (G.M.); 0000-0001-5097-2260 (N.N.); 0000-0003-0055-1569 (S.L.); 0000-0001-7501-5715 (U.D.G.); 0000-0003-4826-0840 (S.Tripathi); 0000-0002-6272-9118 (M.P.S.); 0000-0001-6202-5965 (M.B.); 0000-0002-1141-6189 (A.K.); 0000-0002-7995-0900 (A.J.V.); 0000-0003-0611-8088 (S.Tripathy); 0000-0003-2323-2587 (S.S.); 0000-0001-7951-7595 (A.S.)

Nitrogen (N) limits crop yield, and improvement of N nutrition remains a key goal for crop research; one approach to improve N nutrition is identifying plant-interacting, N_2-fixing microbes. *Rhodotorula mucilaginosa* JGTA-S1 is a basidiomycetous yeast endophyte of narrowleaf cattail (*Typha angustifolia*). JGTA-S1 could not convert nitrate or nitrite to ammonium but harbors diazotrophic (N_2-fixing) endobacteria (*Pseudomonas stutzeri*) that allow JGTA-S1 to fix N_2 and grow in a N-free environment; moreover, *P. stutzeri* dinitrogen reductase was transcribed in JGTA-S1 even under adequate N. Endobacteria-deficient JGTA-S1 had reduced fitness, which was restored by reintroducing *P. stutzeri*. JGTA-S1 colonizes rice (*Oryza sativa*), significantly improving its growth, N content, and relative N-use efficiency. Endofungal *P. stutzeri* plays a significant role in increasing the biomass and ammonium content of rice treated with JGTA-S1; also, JGTA-S1 has better N_2-fixing ability than free-living *P. stutzeri* and provides fixed N to the plant. Genes involved in N metabolism, N transporters, and *NODULE INCEPTION*-like transcription factors were upregulated in rice roots within 24 h of JGTA-S1 treatment. In association with rice, JGTA-S1 has a filamentous phase and *P. stutzeri* only penetrated filamentous JGTA-S1. Together, these results demonstrate an interkingdom interaction that improves rice N nutrition.

INTRODUCTION

Nitrogen (N) is a vital macronutrient for plant growth, but the limited availability of usable N has led to the extensive use of N fertilizers, which are both energy intensive to produce and environmentally unfriendly to use. N fixation, that is the conversion of N_2 to forms the plant can use, provides an attractive alternative to exogenous fertilizers. However, the ability to fix atmospheric N_2 is exclusive to prokaryotes and these N_2-fixing prokaryotes are termed diazotrophs. Moreover, only a monophyletic group of angiosperms of the order Eurosids I interacts with a group of specific diazotrophs to exploit the N fixed by these diazotrophs within symbiotic nodules (Soltis et al., 1995). These findings have prompted the development of synthetic biology approaches to engineer N_2-fixing symbiosis in cereals (Rogers and Oldroyd, 2014).

IN A NUTSHELL

Background: Nitrogen limits crop yield and improvement of nutrition remains a key goal for crop research; one approach to improve nitrogen nutrition is identifying plant-interacting microbes that fix atmospheric nitrogen (N_2) into forms that plants can use, such as ammonium. *Rhodotorula mucilaginosa* JGTA-S1, is a unicellular fungus isolated from the internal tissues of narrowleaf cattail (*Typha angustifolia*). The pink-colored yeast improves the growth of its host cattail and the JGTA-S1 genome contains many genes supporting its life as a plant-associated beneficial fungus. JGTA-S1 could not use nitrate—the most common form of nitrogen available in the soil— and could not convert nitrate and nitrite to ammonium. However, the yeast contains nitrogen-fixing bacteria inside its cells that may help it fix nitrogen. This suggested that JGTA-S1 depends on its host or its endogenous diazotrophs for ammonium.

Question: We wanted to see if JGTA-S1 could use the crop plant rice as host and promote its growth and nutrition, especially nitrogen nutrition. We also wanted to study the role of its endosymbiotic bacteria in controlling yeast and plant growth.

Findings: We found that JGTA-S1 colonizes rice as host and increases growth and nitrogen content in the plant. Biological-nitrogen-fixation is performed by prokaryotes only and involves conversion of atmospheric nitrogen into usable form. JGTA-S1 grows in nitrogen-free media and fixes nitrogen aided by its endosymbiotic nitrogen-fixing bacteria one of which is *Pseudomonas stutzeri*. The endofungal diazotrophs are important for the viability of JGTA-S1 and has important role in increasing biomass and ammonium content of plant treated with the yeast. JGTA-S1 also fixes nitrogen *in planta* and supplies the fixed nitrogen to the plant. In association with plants, the yeast forms filamentous structures which are actively penetrated by *Pseudomonas stutzeri*. We demonstrate a tripartite interaction between endobacteria, yeast JGTA-S1 and rice that improves nitrogen nutrition in plants.

Next steps: Improving nitrogen nutrition in crop plants is a challenge for scientists. It would be interesting to see whether this three-kingdom interaction can be used to improve nitrogen nutrition in plants other than rice, or whether the beneficial role of the endofungal bacteria is plant specific.

In addition to symbiotic species, the role of free-living diazotrophs in improving N metabolism is increasingly being studied (Geurts et al., 2016), as many of these organisms colonize plants as endophytes. For example, many members of the Poaceae derive a significant fraction of their N from biological N_2 fixation (Carvalho et al., 2014); however, N_2 is sequestered at relatively low efficiency through these interactions (Dobbelaere et al., 2003; Carvalho et al., 2014). Other studies have reported that diazotrophs associate with fungi in nature (Gehrig et al., 1996; Wang et al., 2017). Despite this, the importance of the interactions of beneficial fungi with bacteria in plant N metabolism remains to be investigated.

Endophytes are plant-associated microbes that asymptomatically colonize the plant endosphere. The community structure of endophytes in planta is primarily dictated by the soil in which the host plant grows, with plant genotype having only a limited influence (Bulgarelli et al., 2012; Lundberg et al., 2012; Peiffer et al., 2013; Schlaeppi et al., 2014; Edwards et al., 2015). Plants growing in marginal and contaminated environments harbor specialized microbes (Barzanti et al., 2007) with properties that help their hosts cope with deficiencies of critical nutrients. The broad host ranges of endophytes make this host–microbe interaction an exciting area of study, since it opens up the possibility of transmitting the critical properties of endophytes to agriculturally valuable surrogate host plants (Khan et al., 2012; Knoth et al., 2013). Fungal and bacterial endophytes coexist within the plant endosphere, providing a niche for intimate transkingdom interactions. Such interactions are largely ignored in plant–microbe interaction studies.

Many plant-associated fungi serve as hosts to endosymbiont N_2-fixing microbes. These interkingdom interactions may allow the eukaryotes (fungi and, in turn, plants) to make use of the N_2 fixed by the bacterial endosymbionts. For example, *Geosiphon pyriforme*, an arbuscular mycorrhizal (AM) fungus, harbors N_2-fixing *Nostoc* cyanobacteria. Intracellular bacteria have been identified in various mycorrhizal species in nature (MacDonald and Chandler, 1981; Scannerini and Bonfante, 1991) and in the mycorrhiza-like fungus *Serendipita indica*. Gram-negative *Candidatus* Glomeribacter gigasporarum and the recently sequenced Mollicutes-related coccoids (Torres-Cortés et al., 2015) are endosymbionts of AM fungi *Gigaspora margarita* and *Dentiscutata heterogama*, respectively. *Ustilago maydis*, the causative fungus of maize smut disease, maintains N_2-fixing *Bacillus pumilus* as an endosymbiont (Kobayashi and Crouch, 2009; Ruiz-Herrera et al., 2015). *Rhizopus* sp that cause rice blight harbor the rhizoxin-producing bacterium *Burkholderia rhizoxinica* (Partida-Martinez and Hertweck, 2005). The interaction of the human opportunistic pathogen *Candida albicans* with *Pseudomonas aeruginosa* is another example of an interkingdom association (Hogan and Kolter, 2002).

Interkingdom interactions have primarily been studied from the standpoint of pathogenesis (Valdivia and Heitman, 2007), whereas beneficial tripartite interactions have rarely been investigated in detail. One example of such a beneficial interaction in plants is the interaction between an endophytic fungus harboring a viral endosymbiont and tropical panic grass (*Dichanthelium lanuginosum*),

[1] These authors contributed equally to this work.
[2] Current address: School of Interdisciplinary Studies, University of Kalyani, Kalyani 741235, West Bengal, India.
[3] Address correspondence to Anindita Seal (asbcg@caluniv.ac.in).
The author responsible for distribution of materials integral to the findings presented in this article in accordance with the policy described in the Instructions for Authors (www.plantcell.org) is: Anindita Seal (asbcg@caluniv.ac.in).
www.plantcell.org/cgi/doi/10.1105/tpc.19.00385

where the virus–fungus duo confers heat tolerance to the plant (Márquez et al., 2007). An example of a eukaryote that uses the N_2 fixed by a diazotrophic endosymbiont within fungi for nutrition is leafcutter ants of the Amazon ecosystem. The ants grow fungal gardens for food that are enriched in N_2-fixing diazotrophs dominated by *Klebsiella* sp (Pinto-Tomás et al., 2009). Our study shows a similar three-way interkingdom interaction that improves N nutrition of plants.

Rhodotorula mucilaginosa JGTA-S1 was isolated as a shoot endophyte of narrowleaf cattail (*Typha angustifolia*), the predominant flora of a tailings pond associated with a uranium mine in Jaduguda, India (22.65°N, 86.35°E). The tailings pond is a metal-contaminated, highly anaerobic geochemical environment where metal-laden sludge is disposed of following the extraction of uranium ore. JGTA-S1 was one of two endophytic yeast strains isolated from *Typha*, along with 10 other bacterial endophytes (Saha et al., 2016). Endophytic yeasts were previously reported in maize (*Zea mays*), banana (*Musa acuminata*), rice (*Oryza sativa*), tomato (*Solanum lycopersicum*), wheat (*Triticum aestivum*), poplar (*Populus trichocarpa*), and several other plant species (Larran et al., 2001; Cao et al., 2002; Larran et al., 2002; Tian et al., 2004; Nassar et al., 2005; Gai et al., 2009; Xin et al., 2009). None of these yeast strains were shown to have detrimental effects on their plant hosts. JGTA-S1, like *Rhodotorula* yeasts isolated from cottonwood (*Populus trichocarpa*) and hybrid poplar (*P. trichocarpa* × *Populus deltoids*), has important beneficial effects on plant growth (Xin et al., 2009; Sen et al., 2019). *Rhodotorula* are rare unicellular fungi from the phylum Basidiomycota. *R. mucilaginosa* (previously *R. rubra*) promotes mycorrhizal colonization in soybean (*Glycine max*; Sampedro et al., 2004). *Rhodotorula* sp also exhibit biocontrol activity in postharvest apple (*Malus domestica*) and strawberries (*Fragaria ananassa*; Li et al., 2011; Zhang et al., 2014). *R. mucilaginosa* showed enhanced bioprotective effects when used to inoculate rice stems (Akhtyamova and Sattarova, 2013).

Since the publication of the first plant endophytic yeast genome sequence, from *Rhodotorula graminis* WP1 (Firrincieli et al., 2015), the genomes of 22 *Rhodotorula* yeasts have been sequenced, including *R. mucilaginosa* JGTA-S1 (accession number PEFX00000000). The JGTA-S1 genome was recently compared with the genomes of three other *Rhodotorula* yeasts (*R. graminis* WP1, *R.* sp JG1b, and *R. mucilaginosa* C2.5t1) and *Rhodosporidium toruloides* NP11, revealing several unique aspects of its endophytic lifestyle and plant growth-promoting activities (Sen et al., 2019). JGTA-S1 solubilizes mineral phosphate (P), as does the endophytic yeast *R. graminis* (Xin et al., 2009). The genome of JGTA-S1 contains several genes potentially able to promote plant growth due to their roles in producing the plant hormone auxin and several inorganic and organic phosphatases and P-uptake transporters (Sen et al., 2019). Additionally, the JGTA-S1 genome contains the first gene of the cytokinin biosynthesis pathway and a gene encoding isopentenyl-diphosphate Δ-isomerase, an enzyme that converts cytokinin from its inactive to its active form. Biosynthetic genes for abscisic acid, gibberellin, and jasmonic acid and genes responsible for sterol biogenesis and metabolism with the potential to influence the brassinosteroid biosynthesis pathway were also identified in the JGTA-S1 genome (Sen et al., 2019).

In this study, we explored the interaction between JGTA-S1 and rice, as this yeast significantly improves rice growth and N content. Our findings reveal that JGTA-S1 has a dimorphic life cycle in association with plants and harbors a N_2-fixing endobacterium, *Pseudomonas stutzeri*. The fungus–bacterium interaction is critical for the survival of JGTA-S1, and for its ability to fix N_2. JGTA-S1 also fix N_2 in planta and supply N to rice. These findings uncover a beneficial tripartite interaction involving the diazotroph *P. stutzeri*, the yeast JGTA-S1, and the important grain crop rice; this interaction could potentially be used to improve N nutrition in cereals.

RESULTS

Rhodotorula Colonizes Rice Endophytically and Promotes Plant Growth

R. mucilaginosa JGTA-S1 was previously isolated as a shoot endophyte of *Typha*. This fungus, which forms pink colonies, was initially identified by BLAST and phylogenetic analysis of 18S rDNA (KP233783) and *D1/D2* region sequences (KP233784). The JGTA-S1 genome was recently sequenced (accession number PEFX00000000). JGTA-S1 has a substantial plant growth-promoting effect on its host *Typha* (Sen et al., 2019), prompting us to investigate whether it would have a similar effect on rice cv Swarna MTU 7029). The plants were grown on Soilrite containing Murashige and Skoog (MS) medium (N-replete conditions) for these experiments. A Mann-Whitney test for shoot length, root length, and biomass (dry mass) in yeast-treated plants indicated that the effect on plant growth was highly significant (P-value < 0.0001 for dry mass and P-value < 0.0011 for shoot length) and substantial (fold change ~2.8 for dry mass, ~1.3 for shoot length, and ~1.35 for root length) in rice plants at 3 weeks postinfection (wpi; Figure 1A). Similar results were obtained with two other varieties of rice, Bordan and IR64 (Supplemental Figures 1A and 1B).

The fungus attached to the rice root and underwent morphological changes within 24 h, demonstrating that it was completing its life cycle using rice as a host. Binucleated telial cells and diploid thick-walled teliospores were observed both outside and inside root cells within 7 d, which is typical of a Pucciniomycotina (Figure 1B). More than one yeast cell colonized a single root cell (Figure 1C), demonstrating that JGTA-S1 has an endophytic lifestyle.

Microarray Analysis of Early Changes in the Root Transcriptome upon *R. mucilaginosa* Treatment

We performed global transcriptomic analysis to explore the nature of the interaction between rice and JGTA-S1. Since *Rhodotorula* underwent morphological changes within 24 h postinfection (hpi), we analyzed changes in the rice root transcriptome at 24 hpi compared with the 0-h control to gain insight into the early genes regulated in response to JGTA-S1. A cutoff of $\log_2$ (fold change) ≥ 2 or -2 (P-value cutoff, 0.05) was used to identify differentially expressed genes (DEGs) between treatments (Supplemental Data Sets 2 and 3, Gene Expression Omnibus [GEO] accession number

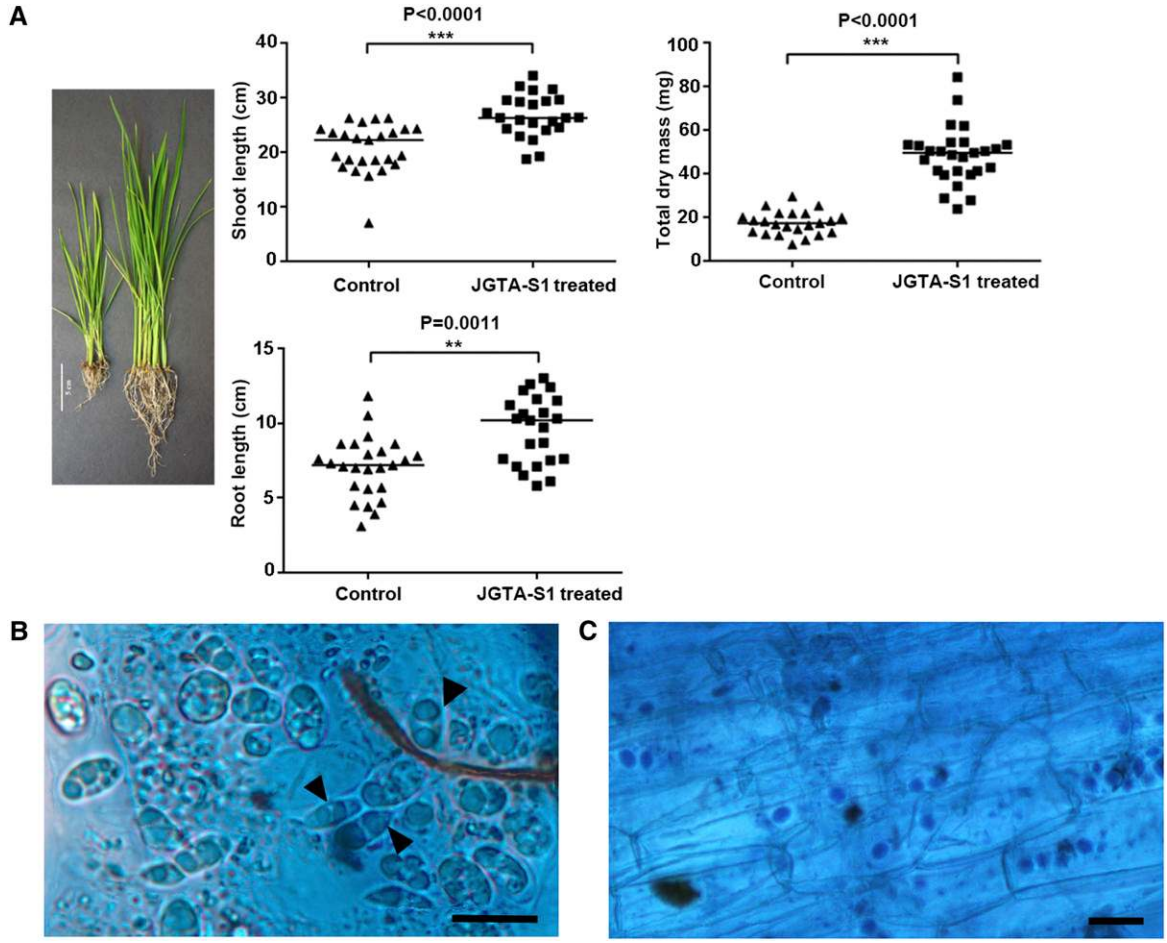

Figure 1. *R. mucilaginosa* JGTA-S1 Associates with Roots and Promotes Plant Growth in Rice.

Four- to 5-d-old rice plants of equal length were grown in Soilrite supplemented with MS medium (N-replete conditions) with or without JGTA-S1. Plant growth was measured at 3 wpi by monitoring.

(A) Shoot length, root length (control, $n = 25$; treated, $n = 23$), and dry mass (control, $n = 23$; treated, $n = 27$). (Left) Digital image of control and treated rice. Bar =5 cm. (Right) Mann-Whitney test for shoot length, root length, and total dry mass values (***P-value < 0.001, **P-value 0.001 to 0.01).

(B) and **(C)** Yeast attached to rice roots or root sections stained with lactophenol cotton blue. Binucleated telial cells attached to rice root cells (see **[B]**, arrowheads). Bar = 5 μm. Yeast cells within the rice root section (see **[C]**). Bar = 10 μm.

GSE99075). We performed gene clustering of all DEGs using the Multiple Experiment Viewer via Pearson correlation analysis. DEGs in plants under the same treatment showed uniform clustering (Supplemental Figure 2). The root transcriptome showed extensive changes compared with that in shoots (GEO accession number GSE64321; Supplemental Data Sets 2 and 3; Saha and Seal, 2015), with 2797 genes differentially regulated within 24 hpi in roots. The microarray data were validated by RT-qPCR of selected genes (Supplemental Figure 3).

We subjected the upregulated and downregulated DEGs to Gene Ontology enrichment analysis using AgriGO (Du et al., 2010). There was clear evidence of the suppression of plant defense responses and apoptosis in the roots at 24 hpi, underscoring the notion that these processes were repressed to promote invasion and colonization (Figure 2A). This observation corroborates the finding that the JGTA-S1 genome contains multiple genes useful for escaping plant defense (Sen et al., 2019). P and N metabolic processes were significantly enriched among the DEGs, indicating that *Rhodotorula* promotes P and N metabolism in rice (Figure 2B). Evidence that JGTA-S1 improves P nutrition was substantiated from the genome data as well as experimentally (Sen et al., 2019), although JGTA-S1 infection did not alter total P content per plant (Supplemental Figure 4).

DEGs Regulated by *R. mucilaginosa* in Rice Roots

Receptor-Like Protein Kinases and Defense-Related Genes

Receptor-like kinases (RLKs) represent major DEGs regulated by JGTA-S1 in rice roots (Supplemental Data Set 4). RLKs are key factors in the recognition of microbe-associated molecular

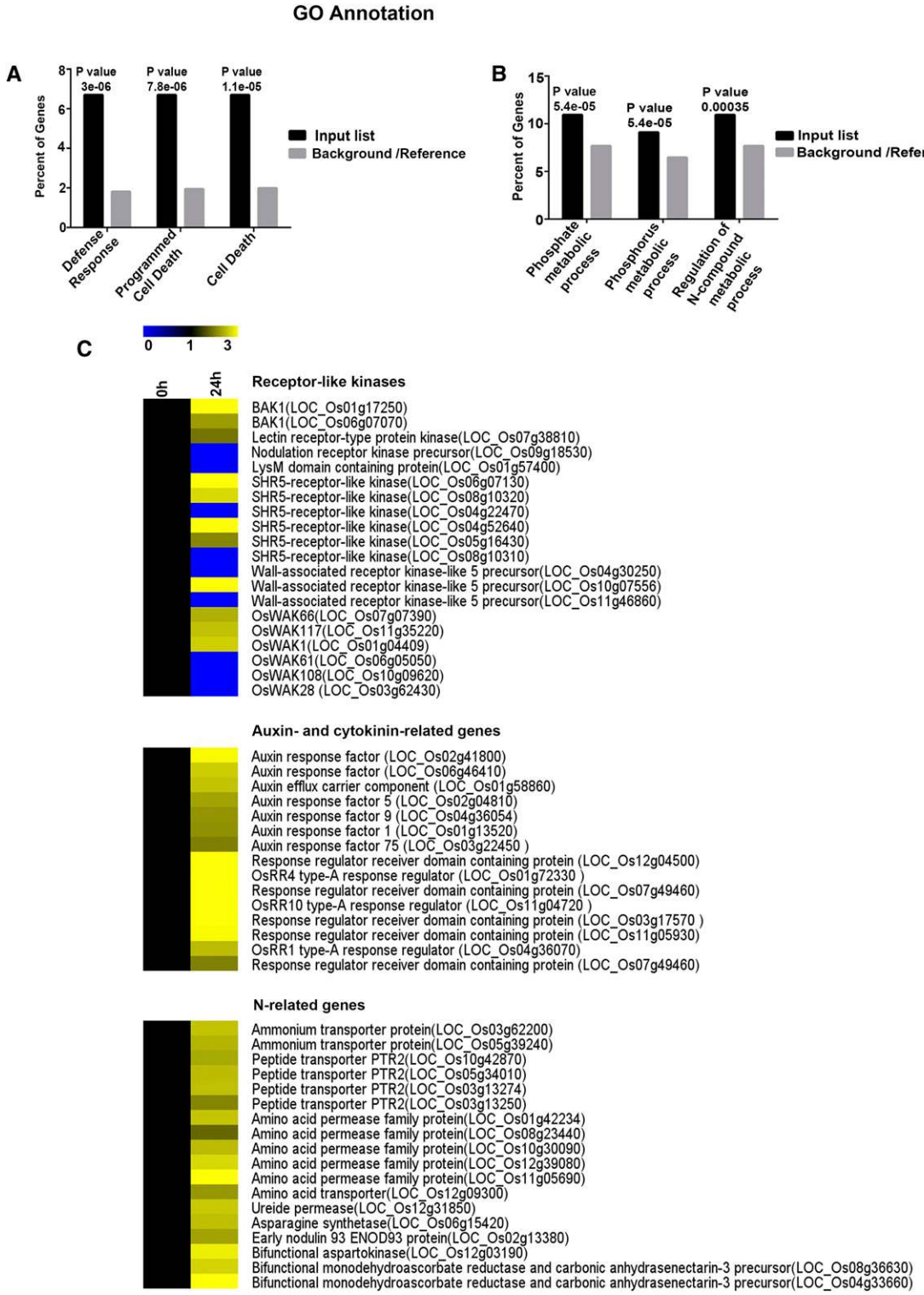

Figure 2. DEGs in Rice in Response to *R. mucilaginosa* JGTA-S1.

(A) and **(B)** Downregulated **(A)** and upregulated **(B)** DEGs in rice roots at 24 hpi were subjected to AgriGO singular enrichment analysis, and enriched categories for biological function were plotted. The P-values indicating significance are listed above the bars; "e" denotes the scientific notation for power of 10. GO, Gene Ontology.

(C) Heatmap of the expression patterns of various genes.

patterns and regulate various processes ranging from plant development to plant defense in response to microbes. Several RLK genes, including genes for wall-associated kinases and members from SHR5-like receptor kinases were differentially regulated in rice roots and shoots (Figure 2C). Three homologs of *BRASSINOSTEROID INSENSITIVE1-ASSOCIATED RECEPTOR KINASE1* were also differentially regulated in a tissue-specific manner. A Cys-rich RLK gene was upregulated in roots, and an S-domain RLK gene was downregulated in roots. A nodulation-dependent receptor kinase precursor was downregulated in roots, and a CLAVATA-like receptor kinase precursor was downregulated in shoots upon JGTA-S1 infection (GSE64321; Saha and Seal, 2015). Genes belonging to the STRUBBELIG-RECEPTOR FAMILY of LRR kinases, which are usually involved in organ development (Chevalier et al., 2005), were upregulated in roots. We identified two LysM domain-containing protein-coding genes, one downregulated in roots and one upregulated in shoots. Putative Subtilisin protease homologs and NBS-LRR and NB-ARC genes implicated in pattern recognition and plant immunity (Pearce et al., 2010; Figueiredo et al., 2014) were also among the DEGs (Supplemental Data Set 4).

Hormone-Related Genes

Auxin- and cytokinin-regulated genes were highly upregulated in rice roots upon JGTA-S1 infection (Supplemental Data Set 4). Auxin response factor and putative cytokinin-regulated type-A response regulator genes were upregulated in roots (Figure 2C). The transcriptome data corroborate the finding that the JGTA-S1 genome sequence contains many genes potentially able to influence hormone signaling in plants (Sen et al., 2019), indicating that this yeast is able to manipulate multiple plant hormonal responses.

Genes Related to N Uptake and Metabolism

JGTA-S1 induced the expression of several genes essential for inorganic and organic N uptake and assimilation in roots. The 0- and 24-h time points represent the same phase in the circadian clock, eliminating the possibility that the up- or downregulation of the genes, especially those related to N metabolism, is diurnally controlled (Gutiérrez et al., 2008) rather than an effect of JGTA-S1 infection. Two ammonium transporter genes were upregulated in rice upon JGTA-S1 infection (Supplemental Data Set 4). Organic N transport appeared to be enhanced as well, as many genes encoding PTR2-like peptide transporters, amino acid permeases, and transporters were upregulated upon JGTA-S1 infection. An *ANT1*-like gene encoding aromatic and neutral amino acid transporter and a ureide permease gene were upregulated upon JGTA-S1 treatment. The upregulation of a ureide permease gene is an interesting finding, as *Rhodotorula* produces urease and can use urea, a commonly used N fertilizer, as the sole N source (Zimmer and Roberts, 1979). The N-assimilation–related DEGs included an Asn synthetase gene, which was upregulated in roots. An *ENOD93* gene was also induced in roots. Among other genes related to N metabolism was a bifunctional aspartokinase gene (Figure 2C).

We searched for N-regulated rice genes described in two recent reports (Obertello et al., 2015 [GSE38102]; Coneva et al., 2014 [GSE61370]) among the JGTA-S1–regulated rice genes. In the GSE38102 experiment, rice plants were supplemented with KNO_3 and NH_4NO_3 and compared with control plants supplied with KCl, while in the GSE61370 experiment, plants were grown under different nitrate regimes. We searched for DEGs regulated $\geq$1.5- or $-$1.5-fold in these studies in our data. Despite significant differences in experimental conditions, many of the N-regulated genes described in these reports, especially those differentially regulated upon N treatments (normal versus induced, GSE61370 or $-$N versus $+$N, GSE38102), were regulated in a comparable manner in our data set (Supplemental Data Sets 5 and 6). This similarity indirectly supports the positive influence of JGTA-S1 on N metabolism in rice.

N-Uptake Genes Exhibit Sustained Upregulation in Roots

The growth-promoting effect of *Rhodotorula* on rice plants became exceedingly prominent at 3 to 4 wpi. We performed RT-qPCR of selected N-uptake and -assimilation genes to measure their expression levels at 3 wpi. The N-transporter genes showed sustained upregulation in JGTA-S1–treated plant roots compared with control roots. The ammonium transporter gene *OsAMT1.1* (*LOC_Os04g43070*) was upregulated in both shoots and roots. *OsNRT2.3a* (*LOC_Os01g50820*), a nitrate transporter gene, was also induced in rice shoots compared with the untreated control. A Gln synthetase gene (*OsGS1-1*, *LOC_Os02g50240*) also maintained increased transcript levels in shoots even after 3 wpi. In roots, *OsNRT2.1* and two *PTR2*-like genes showed sustained upregulation, pointing to a possible increase in N uptake and a persistent N-deficiency signal in the plants triggered by JGTA-S1 treatment (Figures 3A and 3B).

JGTA-S1 Induces the Expression of Four NIN-Like Genes

Four homologs of *NODULE INCEPTION* (*NIN*)–like genes, *LOC_Os11g16290*, *LOC_Os09g37710*, *LOC_Os01g13540*, and *LOC_Os04g41850*, were upregulated upon JGTA-S1 treatment. Only *LOC_Os11g16290* crossed the threshold of twofold induction at 24 hpi. The other genes showed greater than twofold induction at 6 hpi but less than twofold induction at 24 hpi. Although first identified based on their regulatory role in nodulation, transcription factors related to *NIN*-like proteins (NLPs) appear to play central roles in N-(nitrate) metabolism (Ferris and Goodenough, 1997; Konishi and Yanagisawa, 2013; Yan et al., 2016) in nonnodulating plants such as Arabidopsis (*Arabidopsis thaliana*). Excluding *LOC_Os04g41850*, which was upregulated 1.3-fold at 24 hpi, all other *NLP*s were upregulated >1.8-fold in JGTA-S1–treated roots at 24 hpi. This upregulation was sustained even after 3weeks (Figure 3C).

Even though the roles of these rice *NLP* genes in nitrate responses have yet to be determined experimentally, we performed OrthoMCL analysis for comparison of orthologous groups across multiple taxa to gain insight into their likely functions. All four genes clustered into three orthologous groups compared with *Medicago truncatula* and Arabidopsis *NLP*s/*NIN*s (Figure 3D).

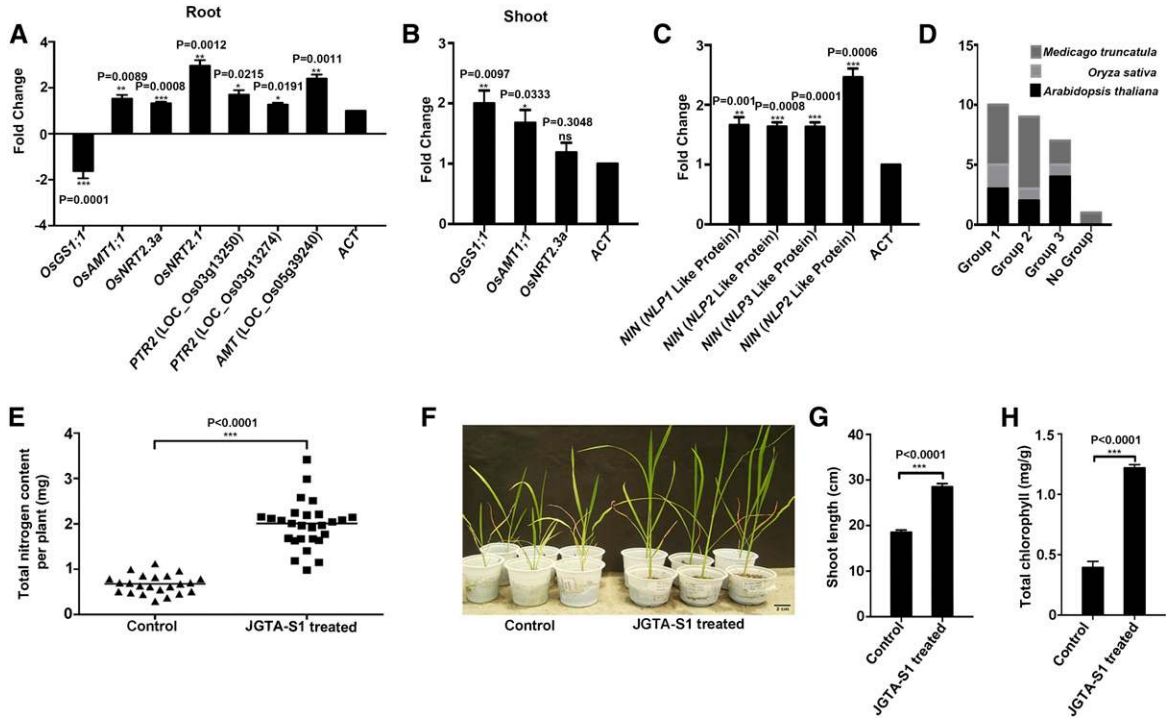

Figure 3. *R. mucilaginosa* JGTA-S1 Improves N Metabolism in Rice.

(A) and **(B)** Rice plants were grown under N-replete conditions and treated with or without JGTA-S1. RNA was isolated from root and shoot tissue at 3 wpi and used for RT-qPCR. Expression levels of N-uptake and -assimilation genes at 3 wpi in **(A)** roots and **(B)** shoots.

(C) Expression levels of rice NIN-like transcription factor genes at 3 wpi.

(D) OrthoMCL clustering of rice NLP genes.

(E) Total N content per plant grown under N-replete conditions, as measured by the Kjeldahl method.

(F) to **(H)** Rice plants grown on artificial soil without N supplementation (low-N conditions). Effect of JGTA-S1 supplementation on rice was monitored compared with the untreated control after 10 DAI. **(F)** Digital image of rice plants. Shoot length **(G)** and chlorophyll content **(H)**. Statistical analysis was performed using Mann-Whitney unpaired two-tailed *t* test. Data are given as mean ± SE.

LOC_Os04g41850.1 and *LOC_Os11g16290.1* were within the same orthologous group as *AtNLP8*, *Medtr2g099350*, and *Medtr4g068000*. *LOC_Os01g13540.1* appears to be orthologous to *AtNLP7*, and *Medtr0022s0430* and *Medtr1g100970*. *LOC_Os09g37710.2* belonged to a group consisting of *AtNLP1*, *AtNLP2*, *AtNLP4*, and *AtNLP5* and *Medtr3g115400*.

JGTA-S1 Infection Increases NUE in Rice

We measured total N levels in three different rice varieties to confirm the effect of JGTA-S1 treatment on N metabolism in rice. The total N content per plant increased significantly (fold change ~2.95) in *O. sativa* cv Swarna MTU7029 (Figure 3E) upon JGTA-S1 treatment. Similar increases were observed for rice varieties IR64 (fold change ~1.77) and Bordan (fold change ~1.97; Supplemental Figures 5A and 5B). Since the amount of N application was identical for all plants, we calculated the relative N-use efficiency (NUE) based on the biomass of JGTA-S1–treated versus control plants (Saha et al., 2016). The relative NUE increased ~2.62-fold upon JGTA-S1 treatment in *O. sativa* cv Swarna MTU7029. These results confirm the notion that JGTA-S1 improves N nutrition in rice, as predicted by the transcriptome data. This increase was independent of the rice variety examined.

JGTA-S1 Improves Rice Growth in Low-N Medium

Nutrient-regulated developmental programs in plants often influence the expression of genes involved in symbiosis. The N-regulated genes control nodulation in legumes (Benedito et al., 2008). The effect of JGTA-S1 on N nutrition was confirmed when plants were grown on low-N medium (Soilrite without supplementation of exogenous N, with or without JGTA-S1). Plants not supplemented with JGTA-S1 were supplied with N-free medium. The untreated plants turned chlorotic within 10 d counting from the day the treated plants were supplemented with JGTA-S1. We evaluated the effects of JGTA-S1 by measuring the shoot length and chlorophyll contents of the plant. Supplementing the rice plants with JGTA-S1 increased the shoot length ~1.5-fold (P-value < 0.0001). Chlorophyll content also significantly increased (fold change ~3.09, P-value < 0.0001; Figures 3F to 3H). The positive effect of JGTA-S1 on N metabolism is a key observation, as analysis of the JGTA-S1 genome indicated that this organism contains an incomplete nitrate assimilation pathway,

suggesting that it is unable to take up nitrate as a N source or convert nitrate and nitrite to ammonium (Sen et al., 2019). However, JGTA-S1 appeared to be unique in its ability to grow in the absence of any nitrogen source, exactly like a diazotroph (Sen et al., 2019), making its effect on N nutrition in rice particularly important to investigate.

JGTA-S1 Exhibits a Dimorphic Life Cycle and Associates with Microbes in Planta

To confirm the endophytic lifestyle of JGTA-S1 in rice, we passed extracts from JGTA-S1–infected surface-sterilized plants through 0.45-μm filters. We incubated the filters as described in Methods until pink foci typical of JGTA-S1 were visible (Figure 4A). The time required for pink foci to appear varied from experiment to experiment and took 14 d or more in cold conditions (5°C). Growing the cold-tolerant JGTA-S1 (Sen et al., 2019) at 5°C provided it with a significant growth advantage over the bacteria associated with JGTA-S1, which were coisolated and difficult to eliminate. The pink JGTA-S1 material formed adherent foci on the filters. Once the foci were visible, we stained part of the material with calcofluor (a fluorochrome that binds to cellulose and chitin in plant and fungal cell walls) or lactophenol cotton blue and observed it under a confocal or bright-field microscope. Extensive filamentous structures with true septate hyphae were observed (Figures 4B and 4C). Directional budding and branching were also observed (Figure 4C, arrowhead). Such filaments were never observed when JGTA-S1 was grown in tryptic soya broth (TSB).

We amplified, cloned, and sequenced a fragment of the 26S rDNA (*D1/D2*) gene specific to JGTA-S1 (213 bp; Figure 4D) from

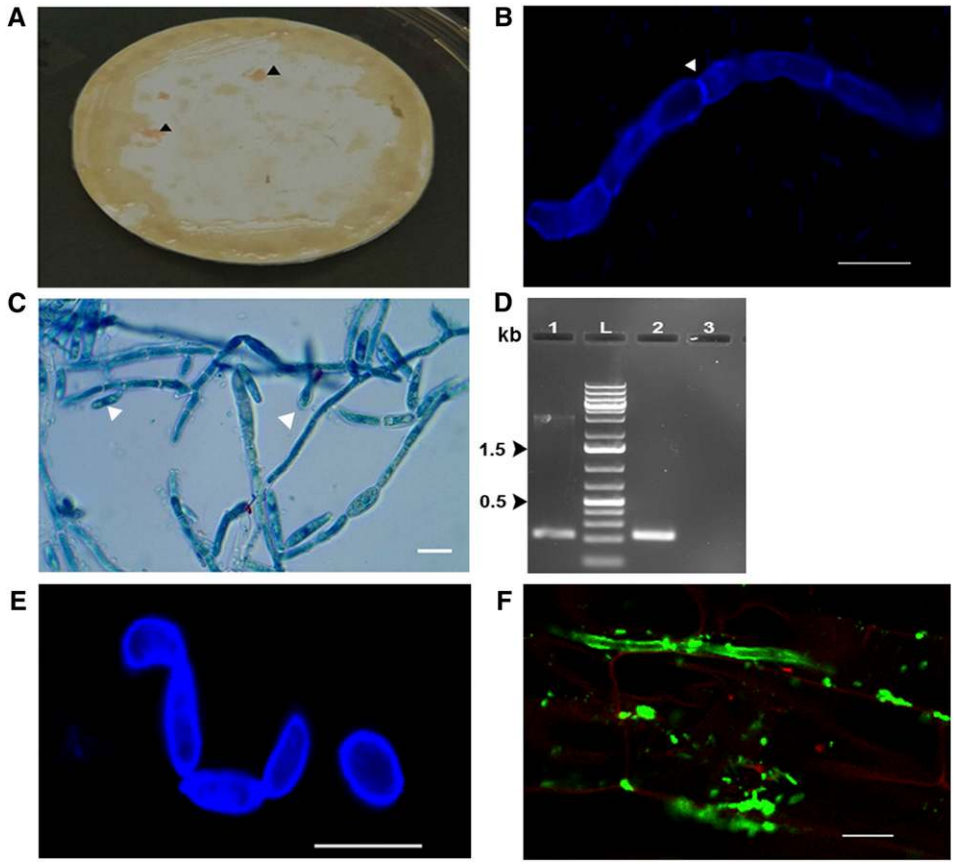

Figure 4. *R. mucilaginosa* JGTA-S1 Shows a Transition from Yeast to Filamentous Form.

Rice plants grown under sterile conditions were supplemented with JGTA-S1. Extracts from surface-sterilized plants were passed through a 0.45-μm filter at 3 wpi. The filters were incubated on PDA plates for 3 d at 30°C, followed by 2 weeks or more at 5°C on PDA plates containing antibiotics.

(A) Pink material on filter paper (arrowhead).

(B) Calcofluor-stained JGTA-S1 showing septate hypha (arrowhead).

(C) Lactophenol cotton blue–stained JGTA-S1 filaments with budding yeast-like structures (arrowhead).

(D) Partial *D1/D2* sequence amplified from genomic DNA isolated from filamentous JGTA-S1 and compared with the yeast form. Lane 1, amplicon from JGTA-S1 in filamentous form; lane L, DNA markers; lane 2, amplicon from JGTA-S1 in yeast form; lane 3, no DNA control.

(E) Calcofluor staining of JGTA-S1 filament induced by FK506.

(F) Rice roots infected with JGTA-S1 at 9 DAI stained with Alexa Fluor 488–labeled WGA and counterstained with propidium iodide. The roots were imaged under a confocal microscope. Bar = 10 μm

the filamentous material to confirm that the hyphae belonged to JGTA-S1. Hyphal growth in the dimorphic fungus *U. maydis* is induced by mating pheromones, low pH, or N starvation (Martínez-Espinoza et al., 1997; Horst et al., 2012). In our case, JGTA-S1 appeared to be haploid, with no evidence of an opposite mating type (Sen et al., 2019). No hyphae formed when the yeast was grown on potato dextrose agar (PDA) plates at low pH or low temperature. Growing the JGTA-S1 cells in N-free medium resulted in the occasional development of chains of fungal cells (Supplemental Figure 6), a prerequisite for pseudohyphae formation (Gancedo, 2001), but this was distinct from the filaments observed when JGTA-S1 was extracted from plants and grown on filter paper.

JGTA-S1 grows quite rapidly in its yeast form. However, the time required to form visible pink foci containing the filamentous form of JGTA-S1 on filter paper following its extraction from the plant indicates that JGTA-S1 likely forms spores inside the plant, which germinate into slow-growing filaments following isolation from the rice endosphere. This finding demonstrates that the JGTA-S1 life cycle includes a dimorphic phase, which was not previously observed in *Rhodotorula* yeasts. Although filament formation was not induced by low pH, N deficiency, or low temperature, treatment with FK506, a specific inhibitor of calcineurin, induced the formation of filament-like structures in JGTA-S1 at a concentration of 1 μg/mL (Figure 4E). This observation confirms the phenomenon of dimorphism in JGTA-S1 and is consistent with the presence of an intact Mating locus in the JGTA-S1 genome, as the Mating locus is often related to the filamentous life cycle of yeasts (Sen et al., 2019).

Byr4 (g3863.t1) and *Cdc16* (g5858.t1; Sen et al., 2019) homologs, which control septation in *Schizosaccharomyces pombe*, were also identified in the JGTA-S1 genome, supporting the notion that JGTA-S1 can form true hyphae. We stained rice seedlings infected with JGTA-S1 with Alexa Fluor 488–labeled wheat germ agglutinin (WGA), which specifically stains the fungal cell wall. JGTA-S1 filaments were observed inside the plant within 9 d after inoculation (DAI), indicating that in nature, filament formation obligatorily requires plant association (Figure 4F).

JGTA-S1 Harbors Multiple Diazotrophic Endobacteria

JGTA-S1 contains an incomplete N-metabolic pathway, yet it grew in N-free medium, whereas a laboratory strain of *S. pombe* did not (Figure 5A). *U. maydis*, the causative agent of maize smut disease, can grow in N-free medium due to the presence of the N_2-fixing *B. pumilus* as an endosymbiont inside the fungus (Ruiz-Herrera et al., 2015). To investigate the presence of a potential N_2-fixing endosymbiont in JGTA-S1, we attempted to amplify *nifH* genes from JGTA-S1 genomic DNA using degenerate primers (Supplemental Figure 7A). Four partial *nifH* sequences (MG566093 to MG566096) were cloned from JGTA-S1. BLASTX analysis of two of these *nifH* sequences (MG566093 and MG566095) showed that they share sequence similarity with genes from the N_2-fixing *Pseudomonas stutzeri* (Supplemental Figure 7B), and with *Bradyrhizobium japonicum* (MG566094) and *Bradyrhizobium* sp (MG566096; Supplemental Figure 7C). Two partial *nifH* sequences amplified from an independent *R. mucilaginosa* strain (JGTA-R1) isolated from *T. angustifolia* roots also share similarity with genes from *Bradyrhizobium* sp (MG566097) and *P. stutzeri* (MG566098; Supplemental Figure 7B), indicating that these results were not artifacts. *P. stutzeri* and *Bradyrhizobium* sp–specific sequences were also found within the unmapped reads of the JGTA-S1 genome (Sen et al., 2019), suggesting that *Bradyrhizobium* sp are another potential endosymbiont of JGTA-S1. Any possibility of contamination was eliminated by subculturing the yeast several times in the presence of antibiotics, followed by microscopy.

Incidentally, we previously isolated a *P. stutzeri* strain (*P. stutzeri*-JGTA-R3) along with the yeast from the *Typha* endosphere (Saha et al., 2016). *P. stutzeri*-JGTA-R3 efficiently colonized rice as an endophyte (Saha et al., 2016). Since no *Bradyrhizobium* strain was isolated, we studied the interaction of JGTA-S1 with *P. stutzeri*-JGTA-R3 in detail. We amplified and cloned full-length *P. stutzeri*–specific *nifH* and *nifD* sequences from JGTA-S1 genomic DNA. Thermal asymmetric interlaced (TAIL)-PCR was used for genome walking to clone the genes flanking the partial *P. stutzeri nifH* sequence using JGTA-S1 genomic DNA as a template. A CDS_8 gene homolog (as per *P. stutzeri* DSM4166 genome annotation) and *nifD* gene homolog flanking the *nifH* gene were amplified, cloned, and sequenced (Figure 5B). We further confirmed the presence of *P. stutzeri* in the yeast by reamplifying, cloning, and sequencing 16S rDNA (primary product 900 bp and nested product of 693 bp; Figure 5C) and *nifH* genes (primary product 603 bp and nested product of 454 bp; Figure 5D) from JGTA-S1 DNA using specific primers for *P. stutzeri*. Reads corresponding to *P. stutzeri* genomic sequences were also found within the raw JGTA-S1 Illumina reads not mapping to the genome (Sen et al., 2019), thereby confirming the notion that *P. stutzeri* is an endosymbiont of JGTA-S1. *P. stutzeri*–specific *nifH* and 16S rDNA sequences were successfully amplified from JGTA-S1 genomic DNA even after a gap of 7 years and several rounds of subculturing, confirming the stability of the association between the fungus and the endosymbiont. *P. stutzeri nifH* was transcribed in JGTA-S1 even when the yeast was grown in complete medium (TSB) containing sufficient organic and inorganic N sources (Figure 5E). Consistent with the presence of diazotrophic endosymbionts, *R. mucilaginosa* JGTA-S1 grew under anaerobic conditions (Supplemental Figure 7D) and fixed atmospheric N_2. JGTA-S1 produced 0.2945 ± 0.0363 nmol of ethylene/h in an acetylene reduction assay, demonstrating why the yeast was able to survive in N-free medium. Transmission electron microscopy revealed bacteria-like structures within the yeast cells (Supplemental Figure 7E).

JGTA-S1 Contains Living Bacteria Inside Its Filaments

We stained the filamentous form of the fungus on filter paper using a LIVE/DEAD BacLight bacterial viability kit. Confocal microscopy revealed live bacteria in the cytoplasm of the yeast filaments (Figure 6A). When isolated from the plant, JGTA-S1 filaments were associated with many bacteria. These bacteria were likely seed-borne, as they were coisolated repeatedly even from untreated plants grown under sterile conditions (as a negative control).

P. stutzeri-JGTA-R3 Penetrates and Becomes Established within *R. mucilaginosa* Hyphae

To investigate whether the *P. stutzeri*-JGTA-R3 strain in our collection was able to associate with JGTA-S1, we incubated green fluorescent protein (GFP)–labeled *P. stutzeri*-JGTA-R3 with *R. mucilaginosa* in both its yeast and filamentous forms. Confocal microscopy revealed no association between the bacteria and the yeast form of JGTA-S1, even after 20 h of coculture (Figure 6B). However, for JGTA-S1 in filamentous form, GFP fluorescence was observed inside the filament (Figure 6C), indicating that *P. stutzeri*-JGTA-R3 was able to invade the fungal filaments. The pink filamentous material on filter paper appeared to be extremely slow growing, with almost no yeast form initially detected. However, after incubation with *P. stutzeri*-JGTA-R3 for 20 h, binucleate asexual spores (Figure 6D, green arrowhead) and cells in yeast form started to bud off of the filaments (Figure 6D, white arrowhead). This phenomenon was not observed in a control experiment in which the yeast was not coincubated with *P. stutzeri*-JGTA-R3. These results suggest that the bacteria promote the transition of the yeast from the hyphal form.

The filamentous form was short lived. After prolonged incubation (4 weeks or more) of filter paper containing filamentous JGTA-S1 on nutrient-rich PDA medium at 5°C, most of the hyphae converted to the fast-growing yeast form, even without coincubation with *P. stutzeri*-JGTA-R3 (Figure 6E). Incubation with *P. stutzeri*-JGTA-R3-GFP at the 4-week time point resulted in accumulation of GFP fluorescence, even inside the yeast form of JGTA-S1, as well as JGTA-S1 filaments (Figure 6E, arrowhead). This finding confirms that the yeast form originated from filaments.

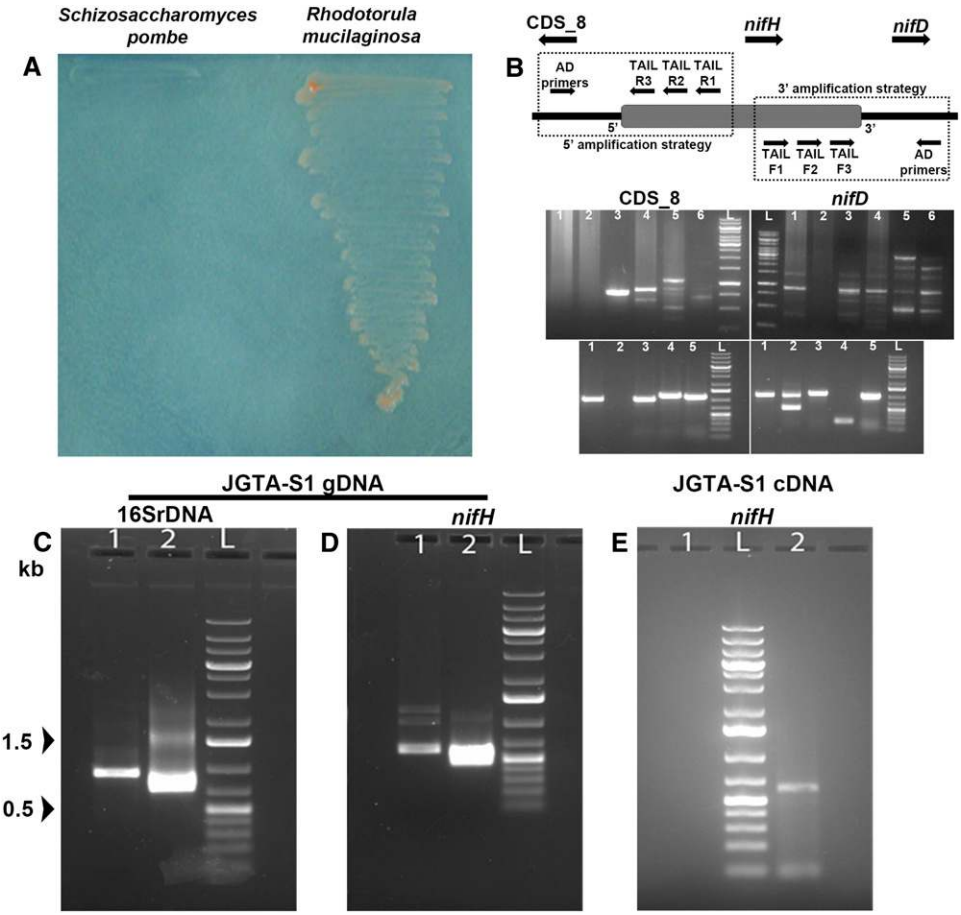

Figure 5. *R. mucilaginosa* JGTA-S1 Contains Bacteria Related to *P. stutzeri* as an Endosymbiont.

(A) JGTA-S1 was streaked onto N-free medium along with a laboratory strain of yeast *S. pombe* D18 h^- to examine its diazotrophic nature.
(B) Flanking genes of *P. stutzeri nifH* from JGTA-S1 genomic DNA amplified using TAIL-PCR. The directions of the genes are represented as in *P. stutzeri* DSM4166. (Top, left) Amplification of the *CDS_8*-homolog. (Top, right) Amplification of the *nifD*-homolog using TAIL R3 or TAIL F3 gene-specific primers together with different AD primers. Lane 1, AD1; lane 2, AD2; lane 3, AD3; lane 4, AD4; lane 5, AD5; lane 6, AD6; lane L, DNA markers. (Bottom) Representative amplicons after colony PCR from putative *CDS_8* and *nifD* clones.
(C) and **(D)** *P. stutzeri* 16SrDNA and *nifH* gene–specific primers were used to amplify *P. stutzeri* 16SrDNA **(C)** and *nifH* **(D)** from JGTA-S1 genomic DNA. **(C)** Lane 1, primary PCR product; lane 2, nested PCR with internal primers. **(D)** Lane 1, primary PCR product; lane 2, nested PCR with internal primer.
(E) RNA was isolated from JGTA-S1 and the cDNA used to amplify *P. stutzeri*–specific *nifH.* Lane 1, no DNA control; lane 2, *nifH* gene amplicon using *nifH* internal primers; lane L, DNA markers.

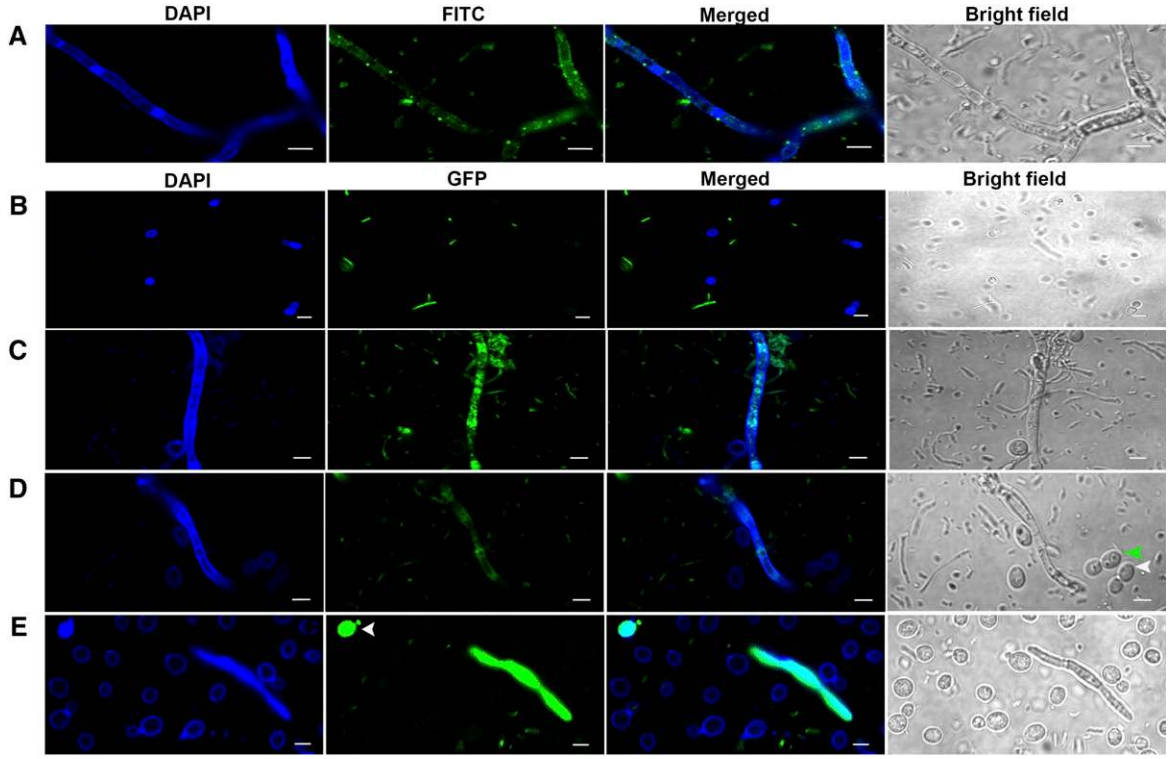

Figure 6. *R. mucilaginosa* JGTA-S1 in Its Filamentous Form, but Not in Its Yeast Form, Associates with Bacteria.

JGTA-S1 filaments were stained with a LIVE/DEAD BacLight bacterial viability kit, counterstained with calcofluor, and imaged by confocal microscopy. DAPI, 4′,6-diamidino-2-phenylindole; FITC, fluorescein isothiocyanate.

(A) JGTA-S1 filament stained with a LIVE/DEAD BacLight bacterial viability kit. JGTA-S1 was incubated with *P. stutzeri*-JGTA-R3-GFP in yeast form or filamentous form.

(B) Microscopy after incubation of *P. stutzeri*-JGTA-R3-GFP with JGTA-S1 in yeast form.

(C) Microscopy after incubation of *P. stutzeri*-JGTA-R3-GFP with JGTA-S1 in filamentous form.

(D) Yeast or spores generated from filaments after incubation with *P. stutzeri*-JGTA-R3-GFP. Arrowheads show JGTA-S1 in yeast (white) and spore form (green). JGTA-S1 isolated from plants maintained for 4 weeks on filter paper at 5°C followed by incubation with *P. stutzeri*-JGTA-R3-GFP.

(E) Arrowhead shows a yeast cell with GFP fluorescence. Bar = 10 μm.

The filamentous form was almost nonexistent after 4 weeks. Despite the abundance of the yeast form, very few cells showed GFP fluorescence, perhaps due to the loss of the GFP plasmid from *P. stutzeri* JGTA-R3-GFP or the unequal vertical transmission of the bacteria into daughter yeast cells, where the amount of labeled bacteria per cell became increasingly diluted in each generation.

Levels of the Endosymbiont *Pseudomonas* in JGTA-S1 Is Crucial for Its Survival

Since *P. stutzeri*-JGTA-R3 isolated from the *Typha* endosphere is sensitive to tetracycline and Timentin, we used these antibiotics to remove this endobacterium from JGTA-S1 cells by repeated streaking. A strain with reduced *P. stutzeri* levels known as strain 11 was previously generated in this manner (Sen et al., 2019). Three other strains were generated from strain 11 by streaking these cells on medium containing the *Bradyrhizobium*-specific antibiotics gentamycin, kanamycin, and carbenicillin (Sen et al., 2019). The objective of these antibiotic passages was to obtain JGTA-S1 strains free of *P. stutzeri* and *Bradyrhizobium* sp.

The antibiotics gentamycin, kanamycin, and carbenicillin were chosen to cure JGTA-S1 of *Bradyrhizobium* sp, as most *Bradyrhizobium* strains are sensitive to these antibiotics (Abaidoo et al., 2002). We performed spotting assays using 59 independent colonies of JGTA-S1 strain 11 (postantibiotic treatment) on N-free medium to screen for yeast strains that showed reduced growth in the absence of any N source (Supplemental Figures 8A and 8B). Three such strains were chosen (Supplemental Figures 8A and 8B, colonies 6, 16, and 38) and named 11.1, 11.2, and 11.3, respectively. We monitored the growth of JGTA-S1 and its derived strains by spotting them onto TSB medium containing both organic and inorganic N sources or on N-free medium. We estimated the growth of the strains as a measure of their fitness. We also measured the relative number of *Pseudomonas*/JGTA-S1 cell by qPCR, where relative *P. stutzeri* 16S rDNA levels were quantified by normalizing against JGTA-S1 *GAPDH* as a reference gene in TSB medium. Cells to be spotted onto TSB plates were grown in TSB medium, and cells to be spotted onto N-free medium were

grown in the presence of ammonium as the sole N source. Strains 11.1, 11.2, and 11.3 were maintained under antibiotic selection so that yeast cells with higher diazotrophic endobacterial levels (*Pseudomonas* or *Bradyrhizobium*) were not selected over those with low endobacterial levels during culture due to their superior growth rates. The plates used for the spotting assay did not contain antibiotics. Strains 11.1, 11.2, and 11.3 were grown in the presence of five antibiotics when grown in liquid TSB, including two for eliminating *P. stutzeri* and three for eliminating *Bradyrhizobium* sp. Only *Bradyrhizobium* sp–specific antibiotics were used when 11.1, 11.2, and 11.3 were grown in N-free plus $(NH_4)_2SO_4$ medium before spotting onto N-free plates because these strains did not survive in the presence of only $(NH_4)_2SO_4$ in the medium when all five antibiotics were used, underscoring the importance of the endobacteria especially in absence of an organic N source. The cells were washed with deionized water and spotted after normalizing the OD_{600} to 0.5. Strains 11.1, 11.2, and 11.3 showed reduced growth irrespective of the medium used compared with the control and strain 11 (Figures 7A and 7B). We previously proposed that the endofungal *P. stutzeri* levels (present per JGTA-S1 cell) respond to the N available to JGTA-S1 (Sen et al., 2019) and are under stringent control in a manner similar to that of the endobacteria of *S. indica* (2–20/fungal cell) and *Candidatus* Glomeribacter gigasporarum (10/spore). The endofungal *P. stutzeri* per JGTA-S1 cell in the 11.1, 11.2, and 11.3*;* increased slightly relative to strain 11 in response to *Bradyrhizobium* sp–specific antibiotics (Figure 7C). These results, together with our earlier findings, indicate that JGTA-S1 endobacteria, some of which are diazotrophs (*P. stutzeri* and *Bradyrhizobium* sp), are important for the growth and viability of JGTA-S1 cells.

The calcium-dependent phosphatase calcineurin regulates morphogenesis in dimorphic fungi (Lee et al., 2013). We therefore treated JGTA-S1 with FK506, a calcineurin inhibitor. FK506 treatment induced the formation of filaments or pseudofilament-like structures from the yeast form, confirming its ability to generate hyphae or pseudohyphae. Therefore, dimorphism in JGTA-S1 appears to be under the control of calcineurin. *P. stutzeri*-JGTA-R3 invaded these artificial filaments in the same manner as natural filaments. This method allowed us to introduce *P. stutzeri*-JGTA-R3 into FK506-treated 11.1, 11.2, and 11.3 strains to create the +Ps strains (Figure 7D). The reduced growth of 11.1, 11.2, and 11.3 on TSB and N-free medium was restored when *P. stutzeri* was reintroduced into these cells (Figures 7A and 7B compare 11.1, 11.2, and 11.3 with the corresponding +Ps strains).

Endosymbiotic *P. stutzeri* JGTA-S1 Plays a Vital Role in Improving N Nutrition in Rice

Among the +Ps strains, we chose 11.3 +Ps (along with strain 11.3) to examine the effect of *P. stutzeri*-JGTA-R3 on plant growth and N nutrition compared to the control JGTA-S1. We applied JGTA-S1, *P. stutzeri*-JGTA-R3, 11.3, and 11.3+Ps to rice to investigate their ability to alter biomass, ammonium content, and nitrate content in plants. The growth rate of strain 11.3 was the lowest, and the growth rate of 11.3+Ps was comparable to that of JGTA-S1 (Figures 7A and 7B).

The use of these different strains of JGTA-S1 with different growth rates allowed us to compare the effects of the endobacterium *Pseudomonas* on N nutrition in rice through this tripartite interaction. We measured biomass, nitrate, and ammonium content in the shoots of plants treated with these *Rhodotorula* strains and *P. stutzeri*-JGTA-R3 compared to the untreated control. The increases in biomass and ammonium content of the rice plants in response to JGTA-S1 were directly related to the fitness of the yeast that, in turn, depended on the endobacterial *Pseudomonas* (Figures 7E and 7G). The 11.3+Ps strain was the most effective at increasing plant biomass and shoot ammonium content, whereas strain 11.3 had no effect on any of the parameters tested.

In an acetylene reduction assay, the N_2-fixing ability of 11.3+Ps did not appear to be significantly higher than that of JGTA-S1, despite a positive shift in the median and mean values of ethylene produced per hour (Figure 7H). However, strain 11.3+Ps had a much better N_2-fixing ability compared with strain 11.3 from which it was derived. The low N_2-fixing ability of 11.3 mirrored its effect on biomass and ammonium content in rice. These results strongly suggest that (1) JGTA-S1 is a much better N_2 fixer than free-living *P. stutzeri*-JGTA-R3 and (2) *P. stutzeri*, an endobacteria of JGTA-S1, played a significant role in increasing both the ammonium content and biomass of rice plants treated with JGTA-S1 (Figures 7E and 7G). We performed an acetylene reduction assay using *S. pombe* D18 h^- (an unrelated fungus) and JGTA-S1 without acetylene injection as negative controls (Figure 7H). Under these conditions, no acetylene reduction took place. We constructed a growth curve of JGTA-S1, 11.3, and 11.3+Ps to quantitatively confirm their ability to grow in the absence of a N source. The JGTA-S1 and 11.3+Ps cells showed similar growth patterns, but 11.3 showed a more prolonged lag phase before reaching the exponential phase. Strain 11.3 also showed a lower growth rate and attained lower growth maxima than the other strains (Figure 7I). This growth curve analysis confirmed the ability of the yeast cells to grow without any external N supply.

Despite the upregulation of *NIN*-like transcription factor genes, potentially indicating a heightened nitrate response, no significant change in nitrate content was observed in JGTA-S1–treated plants versus the controls (Figure 7F). Finally, we measured the N derived from biological N_2 fixation (as $\delta^{15}N$ values) in JGTA-S1–treated plants compared to the untreated controls. This analysis indicated that the yeast-treated plants derived more N_2 from the atmosphere than the controls. This atmospheric N_2 was obtained via biological N_2 fixation, and fixed N was supplied to the rice plants (Figure 7J).

DISCUSSION

NUE is a complex trait governed collectively by the uptake, assimilation, and remobilization of available N in the plant. NUE is an essential parameter for controlling plant yields. Finding ways to improve NUE in plants is crucial for sustainable agriculture, as it would control the indiscriminate use of N fertilizers. Given the inability of most agriculturally important plants to nodulate as legumes do, biological nitrogen fixation by diazotrophic endophytes applied to plants appears to be a useful way to improve N metabolism. The drawback, of course, lies in the fact that biological nitrogen fixation by free-living diazotrophs is much less efficient compared to the efficiency at which rhizobia can fix N_2 within the sophisticated architecture of a symbiotic root nodule.

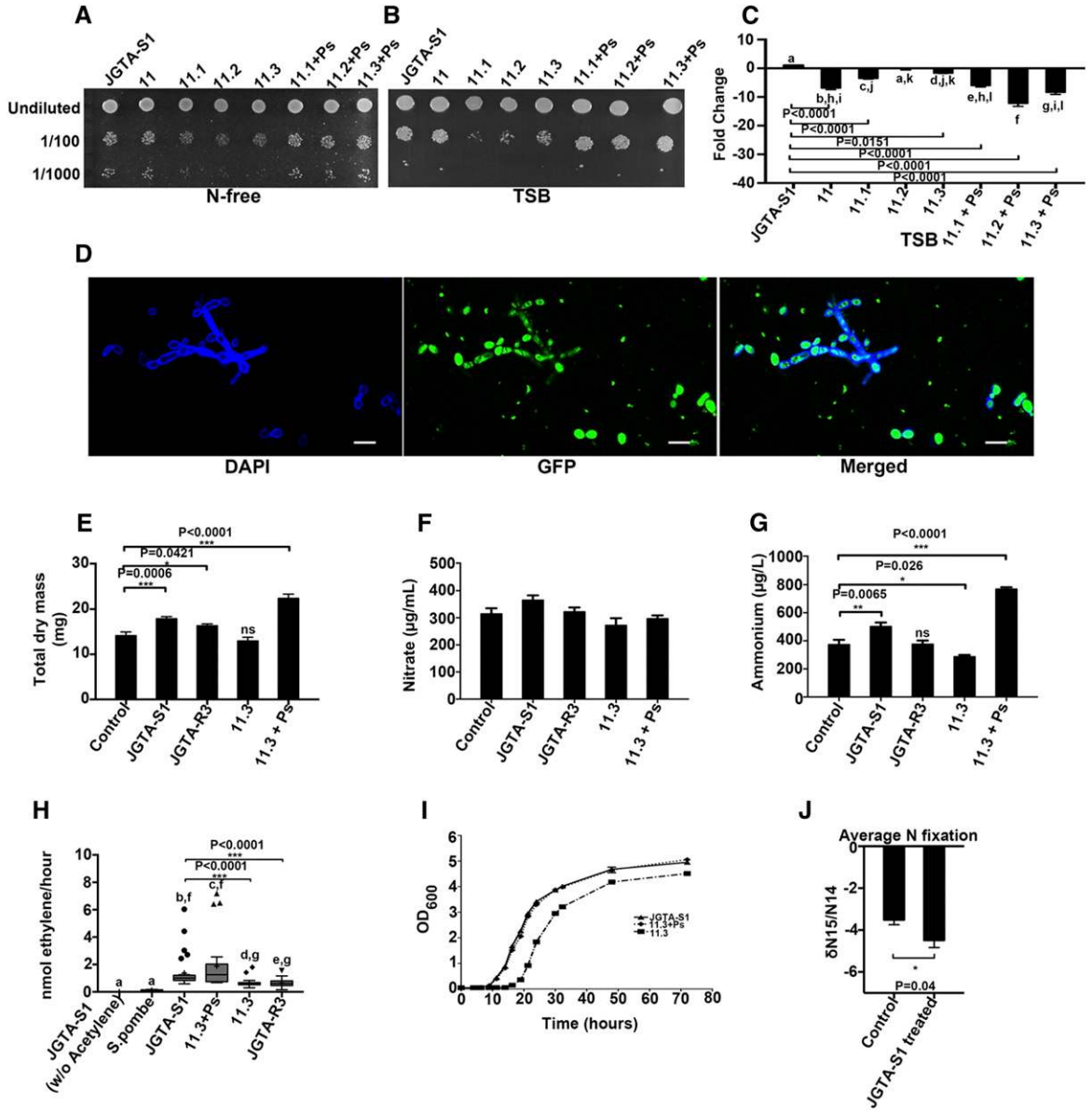

Figure 7. JGTA-S1 Fixes N in Planta, and the Endobacterium *P. stutzeri* Regulates Plant Biomass and Ammonium Levels.

(A) and **(B)** Growth of JGTA-S1 and its derived strains 11.3 and 11.3+Ps was compared in **(A)** N-free medium and **(B)** N-replete TSB.

(C) Relative numbers of *Pseudomonas*/JGTA-S1 cell in these strains were measured by qPCR. Cells were grown in TSB as described in Methods, and relative levels of *P. stutzeri* 16S rDNA gene were quantitated against JGTA-S1 *GAPDH* as a reference gene.

(D) JGTA-S1 treated with FK506 incubated with GFP-labeled *P. stutzeri*-JGTA-R3 for 20 h. *P. stutzeri* outside the yeast was killed with tetracycline and Timentin, followed by confocal microscopy. The effects of JGTA-S1, *P. stutzeri*-JGTA-R3, 11.3, and 11.3+Ps on plant growth and inorganic N content were analyzed. Rice plants were treated with 1× MS (control), JGTA-S1, *P. stutzeri*-JGTA-R3, 11.3, and 11.3+Ps, and plant parameters were measured at 4 wpi. Bar = 10 μm. DAPI, 4′,6-diamidino-2-phenylindole.

(E) to **(G)** Total dry mass **(E)**, nitrate content **(F)**, and ammonium content **(G)**. Statistical comparisons for nitrate content were performed using one-way analysis of variance with Tukey's post hoc test ($n = 3$). Statistical comparisons for ammonium content ($n = 6$) and dry mass (control, $n = 16$; JGTA-S1 treated, $n = 24$; 11.3 treated, $n = 14$; 11.3+Ps treated, $n = 14$; JGTA-R3 treated, $n = 24$) were performed using Kruskal-Wallis nonparametric test followed by Dunn's post correction test.

(H) JGTA-S1, 11.3, 11.3+Ps, and *P. stutzeri*-JGTA-R3 were grown in N-free medium. The OD of the cells was normalized prior to the acetylene reduction assay. *S. pombe* (a nondiazotrophic yeast strain) and JGTA-S1 without acetylene injection were used as negative controls. Statistical analysis was performed using the Kruskal-Wallis nonparametric test followed by Dunn's post correction test (JGTA-S1 without acetylene, $n = 10$; *S. pombe*, $n = 10$; JGTA-S1, $n = 32$; 11.3, $n = 31$; 11.3+Ps, $n = 27$; *P. stutzeri*-JGTA-R3, $n = 31$).

Mycorrhizae are the only fungi reported to improve N nutrition in plants, but the proposed mode of this improvement is increased N supply. AM fungi induce changes in root architecture in rice concurrent with the upregulation of several inorganic or organic N-uptake genes (Gutjahr et al., 2015). However, despite the presence of diazotrophs in the mycorrhizosphere, their participation in the improvement of N metabolism in plants has not been studied (Barbieri et al., 2005, 2007).

The property of N_2 fixation is absent in eukaryotes, but they have circumvented this deficiency by associating with N_2-fixing microbes (Kneip et al., 2007), allowing both partners to exploit challenging niches. Nitrogen appears to be at least one of the critical factors controlling symbiotic and pathogenic fungi–bacteria associations in plants. Examples of interkingdom interactions with the potential to improve N nutrition in the associated eukaryotes include *B. pumilus–U. maydis*–plant, cyanobacteria–*G. pyriforme*–plant (Gehrig et al., 1996), and *Klebsiella* sp–fungi–leafcutter ant interactions. In each of these cases, a fungus (containing diazotrophs) is one of the partners. Such interactions may serve as alternative ways of improving N transfer to the host plant. In the case of the *Allomerus decemarticulatus* (ant)–*Trimmatostroma* sp (fungus)–*Hirtella physophora* (plant) three-way interaction, transfer of N from the fungus to the plant has been demonstrated (Leroy et al., 2017). Various species of the Gigasporaceae AM fungi maintain bacteria from *Burkholderia* genera, which are rich in plant-associated N_2-fixing bacteria (Estrada-De Los Santos et al., 2001). For example, *Azospirillum brasilense* (a member of Burkholderiaceae and an endosymbiont of *G. margarita*) contains a nif operon (Minerdi et al., 2001). The mycorrhiza-like basidiomycete *S. indica* also appears to form close associations with bacteria (Sharma et al., 2008), indicating that such associations are the rule in nature rather than the exception.

The effect of *R. mucilaginosa* JGTA-S1 on rice growth and N nutrition is significant and comparable to that of nodule symbiosis on N nutrition in legumes. Treatment with *R. mucilaginosa* JGTA-S1 resulted in a significant increase in plant biomass and the sustained upregulation of N-metabolism–related genes in rice. While this upregulation could have resulted from induced N deficiency due to an arms race between the plant and the yeast for available N (particularly ammonium), the interaction was not limited to mere upregulation of N-uptake genes. JGTA-S1 treatment did not have any deleterious effects on plant health; instead, it resulted in improved N content and NUE in rice. The yeast efficiently fixed atmospheric N_2, increased free ammonium levels in planta due to the presence of diazotrophs within the yeast, one of which was confirmed to be *P. stutzeri*. *Bradyrhizobium* sp and other diazotrophs are potential JGTA-S1 endosymbionts (Sen et al., 2019) that likely play roles in the JGTA-S1–mediated improvement of N metabolism in plants as well. Since no *Bradyrhizobium* sp was available among the *Typha* endophytes, these interactions could not be confirmed in this study.

Rhodotorula has long been known for its ability to grow in the absence of N (Brown and Metcalfe, 1957). Although the authors did not report any endosymbiont in their study, Firrincieli et al., 2015 reported that *R. graminis* WP1 contains a dinitrogen reductase gene (*nifH*; Knoth et al., 2014).

Eukaryotes exploit different mechanisms to acquire and transmit their endosymbionts. In the case of *Rhizopus*, *B. rhizoxinica* can enter the fungal hyphae actively through a local disruption of the fungal cell wall (Moebius et al., 2014). Vegetative spore formation in *Rhizopus* is compromised in the absence of the endobacteria (Partida-Martinez et al., 2007). The endobacteria facilitate spore formation as a strategy to ensure their vertical transmission. Similarly, mycorrhizal endobacteria are transmitted through spores. The vertical transmission of bacteria to the yeast form was previously observed when JGTA-S1 filaments were mixed with *P. stutzeri*-JGTA-R3. The endobacteria were essential for the survival and propagation of JGTA-S1, as they helped the yeast maintain a bacterial pool despite antibiotic treatments (Sen et al., 2019).

Another important observation is the dimorphic transition from yeast to filamentous form discovered in JGTA-S1. Such transitions are often part of the sexual life cycles of human yeast pathogens *Histoplasma*, *Cryptococcus*, and *Candida*, resulting in the formation of adhesive and invasive filaments inside the host, which help them to penetrate host barriers (Sánchez-Martínez and Pérez-Martin, 2001). This process is triggered by a wide variety of stimuli (Gauthier, 2015). The importance of dimorphism is further highlighted by the finding that it may facilitate the association with bacteria. *Candida* associates with *P. aeruginosa* but only in filamentous rather than yeast form (Hogan and Kolter, 2002). The best-studied examples of dimorphism are found in *C. albicans* and the plant pathogen *U. maydis*, both of which share strikingly similar life strategies with *R. mucilaginosa* JGTA-S1. This filamentous transition is a new observation in *Rhodotorula*, which was previously thought to be an asexually budding yeast. Treatment with the calcineurin inhibitor FK506 induced a filament-like transition in JGTA-S1. Calcineurin was previously demonstrated to be a critical regulator of the dimorphic transition (Lee et al., 2013). Our finding, however, is in contrast to that observed in the dimorphic zygomycetes *Mucor circinelloides*, whose hyphal transition is inhibited by FK506 (Lee et al., 2013). Therefore, the effects of FK506 could vary depending on the fungus or dosage.

JGTA-S1 primarily associated with bacteria in the filamentous form and not in the yeast form, which is similar to reports on the *Candida–Pseudomonas* interaction (Hogan and Kolter, 2002). *P. stutzeri*-JGTA-R3, also isolated from the *Typha* endosphere, entered the *Rhodotorula* hyphae, like *B. rhizoxinica*, which enters *Rhizopus microsporus* filaments (Moebius et al., 2014). These

Figure 7. (continued).

(I) For the growth curve, JGTA-S1, 11.3, and, 11.3+Ps were grown in N-free medium, and OD_{600} was measured at different time points. Mean ± SE was calculated for each time point.

(J) $\delta^{15}N$ stable isotope analysis of rice plants treated with MS (control) and JGTA-S1. Values obtained were statistically analyzed using Student's *t* test ($P \leq 0.05$, $n = 6$). Data are given as mean ± SE.

findings indicate that JGTA-S1 likely acquired the *Pseudomonas* from the endosphere of *Typha* in free-living form, suggesting that its association with the fungus is facultative from the bacterial side. However, this is not the case for yeast, since the loss of the diazotrophic endobacteria had a fitness cost. JGTA-R3 was horizontally acquired and vertically transmitted in spore or yeast form, which budded off the filaments. The association of JGTA-S1 with its endobacteria was remarkably stable, which is in agreement with the recent finding that disrupting endosymbiotic associations with a nutrient amendment is never without fitness costs (Fisher et al., 2017).

Unlike *Rhizopus*, *Ustilago*, or *Candida*, JGTA-S1 appeared to associate with various bacteria within the plant. Despite the conservation of life strategies with other pathogenic fungi of subphylum Pucciniomycotina, JGTA-S1 appears to be beneficial to rice (Sen et al., 2019).

Rice genes transcriptionally responding to *Rhodotorula* included many genes known to be regulated in the plant in its encounter with bacteria. The downregulation of an RLK gene belonging to the SHR5 family is directly related to the plant's interaction with diazotrophs (Vinagre et al., 2006). Several hundred RLK genes are induced in sugarcane (*Saccharum officinarum*) in response to the endophytes *Herbaspirillum* and *Gluconacetobacter diazotrophicus* (Nogueira et al., 2001). The flagellin receptor FLS2 is also induced in response to beneficial interactions (Trdá et al., 2014). These findings point to the existence of additional generic mechanisms by which plants respond to microbes, irrespective of the latter being pathogenic or symbiotic (Vandenkoornhuyse et al., 2015). In this study, homologs of the LRR-RLK *BAK1* were upregulated in rice roots and shoots upon JGTA-S1 infection. BAK1 is a coreceptor protein for the brassinosteroid receptor BRI1 and FLS2. BAK1, which has strong effects on immunity-related genes, was upregulated in rice roots supplemented with N (Obertello et al., 2015). Nutrition, immunity, and symbiosis are closely interconnected, where nutrition is believed to regulate immunity and interkingdom symbiosis (Hiruma et al., 2016; Fisher et al., 2017).

A notable observation was the downregulation of a CLAVATA-like gene in JGTA-S1–treated rice shoots. CLAVATA1 and CLAVATA3 are implicated in shoot-derived systemic suppression of nodulation (autoregulation of nodulation; Reid et al., 2011). Although not proven conclusively, these proteins are also implicated in the autoregulation of mycorrhization (Reid et al., 2011; Staehelin et al., 2011). Whether the systemic downregulation of this CLAVATA-like gene or other CLAVATA-like kinases facilitates the colonization of yeast is an important fundamental issue to investigate. The upregulation of these microbe-related plant genes indicates that the effects of JGTA-S1 on the rice transcriptome could represent cumulative effects of the yeast and bacteria rather than the yeast alone. The observation that *Rhizobium radiobacter*, an endobacterium of *S. indica*, has a growth-promoting effect similar to that of the fungus Sharma et al. (2008) suggests that the beneficial effects of the fungi on the plant are a direct consequence of the endobacteria. The increase in biomass and free ammonium content of plants harboring various JGTA-S1 strains differing in *P. stutzeri* content reveals a similar correlation.

In most terrestrial systems, nitrate is the predominant form of N in the soil. JGTA-S1 contains an incomplete nitrate assimilation pathway, unlike *R. graminis* WP1 and related pink yeasts, making JGTA-S1 dependent on organic and ammonium N for survival even when nitrate is abundant. Additionally, JGTA-S1 was isolated from a mine wetland containing metal-laden sludge, an environment that was likely deficient in available ammonium and organic N, with levels too low for the fungus to maintain its free-living state. These genetic and environmental factors likely made the fungus entirely dependent on the host plant or its endosymbiotic diazotrophs for its N supply. The observation that *P. stutzeri nifH* was expressed in JGTA-S1 even under N-replete conditions indicates that JGTA-S1 uses diazotroph-derived fixed N_2 even when N is abundant in its external environment. The N nutrition–related rice genes upregulated by JGTA-S1 included both N-uptake and -assimilation genes, such as an *ENOD93*-like gene that was upregulated in rice upon JGTA-S1 treatment. The overexpression of an *ENOD93*-like gene increased the NUE and amino acid transport to shoots in rice (Bi et al., 2009). The most significant transcriptomic change in rice upon JGTA-S1 treatment was the sustained upregulation of four *NLP*s, encoding central regulators of the nitrate response (Konishi and Yanagisawa, 2013; Yan et al., 2016). However, the roles of rice NLPs in nitrate metabolism and the contribution of the tripartite interaction to the nitrate response (if any) were not clear. Overall, the yeast appeared to have a complex effect on N metabolism in rice. The yeast acquired N_2 from the atmosphere via biological N_2 fixation (aided by its endosymbionts) and provided the fixed N products to the plant, potentially modulating the nitrate response (although not the nitrate concentration per se) and upregulating inorganic and organic N-uptake genes in the plant.

Collectively, the novel tripartite interaction involving *R. muculaginosa*-JGTA-S1, its endosymbiont diazotroph *P. stutzeri*, and rice uncovered in this study improves the NUE in rice, and *P. stutzeri* plays a vital role in this phenomenon. JGTA-S1 was more competent as an N_2 fixer than free-living *P. stutzeri*, thereby making JGTA-S1 a better plant growth-promoting endophyte. It is tempting to speculate that the environment within JGTA-S1 facilitates the N_2 fixation of *P. stutzeri* in a manner similar to the N_2 fixation of *Rhizobium* within the root nodule. *Rhodotorula* is axenically culturable and fast growing, and its microbiome could potentially be synthetically designed. The implications of such interactions are great, paving the way for improving N metabolism in non-nodulating plants of agricultural importance without the need for genetic manipulation.

METHODS

Isolation and Identification of *R. mucilaginosa* JGTA-S1 from Plants

Rhodotorula mucilaginosa JGTA-S1 was isolated from surface-sterilized *Typha angustifolia* shoots as described by Saha et al. (2016). After sterilization, 100 μL of solution from the last wash was plated as a negative control. Debris was removed from the extract obtained from surface-sterilized plants and plated. The plates were incubated for 3 d at 30°C. Pink *Rhodotorula* colonies were repeatedly streaked onto TSB agar plates to obtain a pure culture. To isolate JGTA-S1 from rice, plants were grown in sterile glass jars containing Soilrite (Keltech Energies) mixed with 1× MS medium, pH 6. Extracts from surface-sterilized plants at 3 wpi were passed

through a 0.45-μm filter. The filters were incubated on PDA plates for 3 d at 30°C and transferred to new PDA plates containing carbenicillin (100 μg/mL) and Timentin (250 μg/mL). The plates were incubated at 5°C for 2 weeks or until pink growth of *Rhodotorula* was visible. The pink material was stained with calcofluor and observed under a confocal microscope (FluoView 1200, Olympus). Genomic DNA was isolated from the filaments as described by Bolano et al. (2001). Primers were designed to amplify a JGTA-S1–specific fragment of the 26SrDNA or *D1/D2* gene. Primer sequences are given in Supplemental Data Set 7. The amplified product was cloned and sequenced.

R. mucilaginosa Growth in N-Free Medium

To investigate growth on N-free medium, *R. mucilaginosa* JGTA-S1 and *Schizosaccharomyces pombe* D18 h^- (negative control) were streaked onto Norris Glucose Nitrogen Free Medium (Himedia India) and incubated at 30°C for 7 d.

Plant Growth and Treatments

Rice (*Oryza sativa* cv Swarna MTU7029, Bordan, or IR64) seeds were surface sterilized and germinated on filter paper. Four- to 5-d-old seedlings of equal length were transferred to Soilrite containing 2× MS salt mixture (N-replete conditions, 15 mL of medium/30 g of soil) with (10^7 cfu JGTA-S1 suspended in 10 mL of 1× MS) or without JGTA-S1 unless otherwise mentioned. Control plants were supplied with MS only. Plants were grown in a climate-controlled room under a 24-h cycle consisting of 16 h of light at 30°C and 8 h of dark at 25°C at a humidity level of 70%. Plants were harvested at 3 wpi and used to measure root and shoot length (control, n = 25; treated, n = 23 from three independent experiments) or biomass (control, n = 23; treated, n = 27 from two independent experiments). Tissue from each plant was treated as an independent biological replicate. Plant samples were dried at 60°C for 48 h before measuring the dry weight. For microarray analysis, roots were harvested from 10 3-week-old plants at 0 or 24 h posttreatment with JGTA-S1, frozen in liquid nitrogen, and stored at −80°C. These pooled tissues were treated as independent biological replicates. To assess plant growth without exogenous N supplementation (low N), plants were grown in Soilrite supplemented with N-free medium as described by Saha et al. (2016). JGTA-S1 or N-free medium (low N) was added dropwise around the roots of 5-d-old plants. Plant parameters were measured at 10 DAI. Tissue from each plant was treated as an independent biological replicate (n = 18). To measure chlorophyll content, 400 mg of fresh leaf tissue was extracted overnight in 8 mL of 80% (v/v) acetone, and the absorbance at 645 and 663 nm was measured using a UV-2450 UV-visible spectrophotometer (Shimadzu). Total chlorophyll was calculated as total chlorophyll (mg/g) = 20.2 (A_{645}) + 8.02 (A_{663}) × V/1000 × 1/W (Arnon, 1949).

RNA Isolation

For microarray analysis, RNA was isolated in two replicates each from pooled root tissue obtained from 10 plants. Total RNA was isolated from the frozen tissues using a HiPurA Plant and Fungal RNA Miniprep Purification Spin Kit (Himedia India). The RNA was treated with DNase I (1 unit/2 μg of RNA, Thermo Fisher Scientific) to remove genomic DNA contamination.

Microarray Hybridization and Analysis

Total RNA isolated from rice roots (*O. sativa* cv Swarna MTU7029) was used for microarray analysis. The analysis was performed using an Affymetrix GeneChip Rice St 1.0, corresponding to 146,918 probes representing 41,770 known genes, expressed sequence tags, or clusters (with 15 median probes per gene) following the manufacturer's protocol. The genes were functionally classified based on the complete genome sequence of *O. sativa* cv *japonica* in the Rice Genome Annotation Project (rice.plantbiology.msu.edu), the National Center for Biotechnology Information database, and the European Bioinformatics Institute database (*O. sativa* cv *indica*). Ensemble Plant and Phytozome 11 Biomart and RAP_DB tool (rapdb.dna.affrc.go.jp) were used to complete the annotation and to identify *O. sativa* cv *japonica* homologs of the genes.

RT-qPCR Analysis

RNA was isolated in three biological replicates. Each biological replicate contained root and shoot tissue pooled from 10 plants. Two micrograms of total RNA (as measured in a NanoDrop spectrophotometer, Thermo Fisher Scientific) was used to synthesize cDNA with Random Hexamer Primer (Fermentas) using RevertAid Reverse Transcriptase (200 units/2 μg of RNA, Fermentas) as per the manufacturer's protocol. To validate the microarray data, 0- and 24-h–treated samples were used. To study the differential expression of genes related to N metabolism, RNA was isolated from plants at 3 wpi and compared with RNA from the uninfected controls. Each 10-μL RT-qPCR contained 5 μL of DyNAmoColorFlash SYBR Green I Master Mix (Thermo Fisher Scientific), 0.5 μM each primer, and 25 ng of cDNA. RT-qPCR was performed using a StepOnePlus real-time PCR machine (Applied Biosystems). The thermal step-up was 10 min at 95°C, followed by 40 cycles of 15 s at 95°C and 1 min at 60°C. Data analysis was performed using ExpressionSuite software v1.0.4 (Applied Biosystems). Fold change of expression was calculated using the $2^{-\Delta\Delta Ct}$ method and plotted relative to the control using Prism 5.02 (GraphPad Software). Primer sequences are given in Supplemental Data Set 7. Primer efficiencies were checked using LinRegPCR version 2016.0 (Ramakers et al., 2003).

Predicting Rice Orthologs of *NIN*-Like Genes

Arabidopsis (*Arabidopsis thaliana*) orthologs of *O. sativa* NLP genes up-regulated by JGTA-S1 were predicted using OrthoMCL (Li et al., 2003) and grouped into an orthologous group with Arabidopsis and Medicago sequences.

Measuring Total N Content and Relative NUE

Oven-dried (60°C overnight) plant samples were ground into a fine powder and digested with concentrated H_2SO_4 (Merck), and total N concentration was estimated by the Kjeldahl method in a KEL PLUSKES digestion and Distyl EMVA distillation unit (Pelican). The same amount of N was added to the soil for the control. The relative NUE of JGTA-S1 was measured as described by Saha et al. (2016) by calculating the ratio of the biomass of control (n = 23) and treated plants (n = 27); n represents individual plants.

Amplification of *P. stutzeri nifH*, Flanking Regions, and 16S rDNA Sequences from JGTA-S1 Genomic DNA

Partial *nifH* genes were amplified from *R. mucilaginosa* JGTA-S1 genomic DNA strictly under sterile conditions according to Steward et al. (2004). The products were cloned into the pJET1.2 vector (Thermo Fisher Scientific) according to the manufacturer's protocol and sequenced. Full-length *P. stutzeri nifH* was cloned from JGTA-S1 genomic DNA as a template using modified TAIL-PCR (Liu et al., 1995). Arbitrary degenerate primers (AD1 to AD6) and *nifH* gene–specific primers (TAIL F1 to F3 and TAIL R1 to R3) were used in the primary and secondary PCR. The secondary PCR product was used as a template to amplify the 5′ and 3′ ends of the *P. stutzeri nifH* gene using specific forward and reverse primers. The flanking genes of *P. stutzeri nifH* were cloned by standard TAIL-PCR using JGTA-S1 genomic DNA as a template. The tertiary PCR products were cloned directly into pJET1.2 and sequenced. For specific amplification of *P. stutzeri* 16S rDNA and *nifH*

sequences, primers were designed using the Primer-BLAST program (Ye et al., 2012). For *nifH* RT-PCR, total RNA was isolated from *R. mucilaginosa* cells grown in TSB medium using a Hipura Plant and Fungal RNA Isolation Kit. The RNA was treated with DNase I to remove genomic DNA prior to cDNA synthesis with Random Hexamer Primer and RevertAid RT enzyme. RT-PCR was performed using *P. stutzeri*–specific *nifH* primers. A reaction was conducted without reverse transcriptase to ensure the absence of DNA contamination. A negative control without DNA template was conducted whenever bacterial genes were amplified from JGTA-S1 DNA.

RNA Isolation and Amplification of *P. stutzeri nifH* from JGTA-S1

Total RNA was isolated from JGTA-S1 cells using the TRIzol method (TRIzol reagent, Invitrogen) as described previously (Sen et al., 2019). The RNA was subjected to DNase I treatment and transcribed to cDNA with Moloney Murine Leukemia Virus reverse transcriptase and random hexamers (Thermo Fisher Scientific) per the manufacturer's protocol. cDNA (6.2 ng) was used to amplify *P. stutzeri nifH*. The RT-PCR cycle was 5 min at 98°C followed by 40 cycles of 30 s at 98°C, 15 s at 62°C, and 19 s at 72°C with a final extension of 7 min at 72°C. Minus RT and minus DNA controls were performed as described above.

Acetylene Reduction Assay

The acetylene reduction assay was performed using a gas chromatography with flame ionization detector system (Shimadzu GC-2010 equipped with HP-PLOT 'S' Al_2O_3 50 m, 0.53-mm column; Agilent Technologies). JGTA-S1 without the injection of acetylene and *S. pombe* D18 h^- (an unrelated nondiazotrophic yeast) were used as negative controls. JGTA-S1 and other strains were grown at 30°C for 48 h in TSB medium, and *S. pombe* D18 h^- cells were grown in YES medium. Approximately 10^7 cells were centrifuged, washed twice with sterile water, suspended in 100 μL of sterile water, and used to inoculate 5 mL of N-free medium (for JGTA-S1 cells: Glc, 5 g; yeast extract, 0.1 g; $CaCl_2$, 0.15 g; Na_2MoO_4, 0.005 g; $MgSO_4 \cdot 7H_2O$, 0.2 g; $FeSO_4 \cdot 7H_2O$, 0.04 g; K_2HPO_4, 0.5 g; $CaCO_3$, 1.0 g; and distilled water to 1 L, pH 7.0) and YES medium (for *S. pombe* D18 h^- cells) that had been grown for 72 h at 30°C. The cells were harvested and cell number determined, and 10^7 cells were inoculated in N-free medium (same as above with 3 g/L Phytoagar [Duchefa]) in 16-mL airtight glass vials and sealed with Suba-Seal septa (Sigma-Aldrich). One milliliter of pure acetylene gas was injected through the Suba-Seal septa and incubated for 4 h without shaking. Ethylene production was measured by gas chromatography. JGTA-S1 cells were grown from six different cultures and maintained separately for the biological replicates, with each set containing three to six technical replicates. The total number of replicates was denoted as n. Results represent data for a total of $n = 10$ experiments for JGTA-S1 without acetylene, $n = 10$ for *S. pombe* D18 h^-, $n = 32$ for JGTA-S1, $n = 27$ for 11.3+Ps, $n = 31$ for 11.3, and $n = 31$ for *P. stutzeri*-JGTA-R3.

Effect of N Deficiency and Low pH on *R. mucilaginosa*

Morphological variation of JGTA-S1 due to N depletion was examined by growing the cells on the same N-free medium used for the C_2H_2 reduction assay for 7 d. The effect of pH was checked by growing the cells on PDA at different pH levels (pH 3, 3.5, 4, and 4.5) maintained using citrate buffers of the same pH.

Staining of JGTA-S1 Filaments and Interaction with Endobacteria

Plants were grown in a sterile environment with or without JGTA-S1 treatment. The extract from surface-sterilized 3 wpi plants (Saha et al., 2016) was passed through 0.45-μm filters as described above. The pink material that formed on filter paper was suspended in 1× PBS with (when interaction with *P. stutzeri*-JGTA-R3-GFP was studied) or without tetracycline. The JGTA-S1 filaments were stained with calcofluor. To induce filament formation, 1 μg/mL FK506 (Tacrolimus, Panacea Biotech) was added to TSB broth while growing the fungus. The cells were imaged 3 DAI. Alexa Fluor 488–labeled WGA or lactophenol cotton blue was used when the colonization of JGTA-S1 in planta was studied. For WGA staining, seedlings infected by JGTA-S1 were infiltrated with Hank's balanced salt solution buffer containing 5 μg/mL WGA and incubated overnight in the dark at room temperature. The plant root was counterstained with propidium iodide (excitation, 559 nm and emission, 570 to 670 nm) and imaged under a confocal microscope using an Alexa Fluor 488 filter (excitation, 473 nm and emission, 485 to 545 nm). To visualize endobacteria, the filament was stained with a LIVE/DEAD BacLight bacterial viability kit, counterstained with calcofluor, and observed under a confocal microscope with 4′,6-diamidino-2-phenylindole (excitation, 405 nm and emission, 425 to 460 nm) and fluorescein isothiocyanate filters (excitation, 473 nm and emission, 485 to 545 nm). To study *P. stutzeri* and JGTA-S1 interaction, *P. stutzeri*-JGTA-R3-GFP was grown overnight in the presence of tetracycline (10 μg/mL). *P. stutzeri* cells were mixed with the yeast filaments and incubated at 20°C for 20 h without shaking. The JGTA-S1 in yeast form was similarly mixed with *P. stutzeri*-JGTA-R3-GFP. The cells were counterstained with calcofluor and observed under a confocal microscope with 4′,6-diamidino-2-phenylindole and GFP (excitation, 473 nm and emission, 485 to 585 nm) filters.

Creating Endobacteria-Free JGTA-S1 Cells and Reintroducing Endobacteria

JGTA-S1 strains cured of endobacteria were created as described in Sen et al. (2019). In short, JGTA-S1 cells were streaked five times in N-free medium with 5 g/L $(NH_4)_2SO_4$ in the presence of tetracycline (10 μg/mL) and Timentin (250 μg/mL) to obtain strain 11. Strain 11 was streaked in the presence of 30 μg/mL gentamycin, 50 μg/mL kanamycin, and 100 μg/mL carbenicillin in the same medium. Single colonies of JGTA-S1 were revived once by growing them on TSB plates without antibiotics followed by another round of streaking in the presence of gentamycin, kanamycin, and carbenicillin (Sen et al., 2019). Fifty-nine colonies obtained in this manner were screened by growing them in N-free medium plus $(NH_4)_2SO_4$, followed by spotting onto N-free medium (after normalization to OD_{600} at 0.5) to search for strains whose growth was significantly reduced compared to the control (this study). To reintroduce *P. stutzeri* into strains 11.1, 11.2, and 11.3 and to obtain strains 11.1+Ps, 11.2+Ps, and 11.3+Ps, respectively, strains 11.1, 11.2, and 11.3 were grown in the presence of 1 μg/mL FK506 for 3 d, mixed with *P. stutzeri*-JGTA-R3 (Ps) for 20 h, and plated onto medium containing tetracycline (10 μg/mL) and Timentin (250 μg/mL) to remove any free *Pseudomonas* (this study).

Estimating the Fitness of Endobacteria-Cured Cells

Control and 11.1, 11.2, 11.3, 11.1+Ps, 11.2+Ps, and 11.3+Ps strains were grown in N-free medium plus $(NH_4)_2SO_4$ or TSB medium with or without antibiotic treatment as described below. All media were prepared in 18.3 MΩ water. The 11.1, 11.2, 11.3 cells were grown in the presence of five antibiotics, tetracycline (10 μg/mL), Timentin (250 μg/mL), gentamycin (30 μg/mL), kanamycin (50 μg/mL), and carbenicillin (100 μg/mL), when grown in TSB before they were spotted onto TSB. When the cells were spotted onto N-free medium, the cells were grown in N-free medium supplemented with $(NH_4)_2SO_4$ in the presence of three antibiotics, gentamycin, kanamycin, and carbenicillin, at the same concentrations. Control, strain 11, and the +Ps strains in which *P. stutzeri* was reintroduced were grown without antibiotics. In all cases, the pellets were suspended and washed twice with deionized water before spotting to remove any carried-over medium. The OD_{600} was normalized, and the cells were

spotted onto TSB or N-free medium at different dilutions (undiluted [OD_{600} of 0.5], 1:100, 1:1000).

Estimating the *P. stutzeri* Concentration per JGTA-S1 Cell

To estimate *P. stutzeri* levels per yeast cell, qPCR was performed. Genomic DNA was isolated from JGTA-S1 (control), 11.1, 11.2, 11.3, 11.1+Ps, 11.2+Ps, and 11.3+Ps strains grown in TSB. Cells were grown in the presence of five antibiotics as described in the previous section. A *P. stutzeri*–specific 16S rDNA primer was designed using primer BLAST software, with *P. stutzeri* DSM 4166 as the organism. An equal amount of genomic DNA was used for qPCR. Ten microliters of qPCR reaction contained 5 μL of DyNAmoColorFlash SYBR Green I Master Mix (Thermo Fisher Scientific), 0.5 μM of each primer, and 1.5 ng of genomic DNA. The nucleic acids were measured using Qubit assay kits. qPCR was performed in a 7500 real-time PCR machine (Applied Biosystems). The thermal step-up was 10 min at 95°C, followed by 40 cycles of 15 s at 95°C, 30 s at 60°C. The fold change was calculated by $2^{-\Delta\Delta Ct}$ method using JGTA-S1 *GAPDH* gene as a reference gene. The results correspond to four independent biological replicates. Each qPCR was done in triplicate (experimental replicate). The primer efficiencies were checked using LinReg PCR 2017.1.0.0 software and found to be >90 for every primer pair. Primer sequences are given in Supplemental Data Set 7.

Measuring Dry Mass and Nitrate and Ammonium Contents in Rice Shoot Tissue

Seven-day-old rice plants were grown in N-replete medium and treated with JGTA-S1, *P. stutzeri*-JGTA-R3 (10^6 cfu/plant), 11.3, and 11.3+Ps strains as described above. Control plants were treated with 1× MS only. The treatments were repeated at 3 wpi, after which the plants were grown for an additional week. Shoot tissue from two individual plants was dried and pooled as a single biological replicate for nitrate measurements. Three such replicates ($n = 3$) were used. Experiments were performed in triplicate from each of these replicates. Nitrate was estimated as described by Cataldo et al., (1975), with the following modifications. Ten milligrams of dried shoot tissue was extracted in 1 mL of deionized water and incubated at 45°C for 1 h with intermittent vortexing. The sample was centrifuged, and 20 μL of the supernatant was mixed with 80 μL of 5% (w/v) salicylic acid and 1.9 mL of 2 N NaOH. The absorbance at 410 nm was measured in a spectrophotometer against a standard curve with known concentrations (0 to 300 μg/mL) of KNO_3. Salicylic acid was omitted from the negative controls. Six individual plants were used as a biological replicate ($n = 6$) for ammonium measurements. The experiments were performed in triplicate. Free ammonium was measured from 100 mg of fresh shoot tissue that had been snap-frozen in liquid nitrogen and stored at −80°C. The tissue was homogenized in liquid nitrogen and combined with 1 mL of water. The extract was incubated at 80°C for 10 min, followed by centrifugation at 4000 rpm for 30 min at 4°C. Forty microliters of phenol-alcohol reagent (10% [v/v] phenol in 95% alcohol), 40 μL of freshly prepared sodium nitroprusside, and 100 μL of oxidizing solution (Koroleff, 1976) were added to 1 mL of supernatant and incubated for 2.5 h in the dark at room temperature. The OD_{630} was measured, and ammonium was quantified against known amounts of $(NH_4)_2SO_4$ as described previously (Koroleff, 1976). For dry mass measurements, plant shoot tissue was dried at 60°C for 5 d and weighed. The number of plants was as follows: control, $n = 16$; JGTA-S1 treated, $n = 24$; 11.3 treated, $n = 14$; 11.3+Ps treated, $n = 14$; and JGTA-R3 treated, $n = 24$, where n represents individual plants.

Growth Curve Analysis of JGTA-S1 and Its Derived Strains

Three independent cultures of JGTA-S1, 11.3, and 11.3+Ps were grown in N-free medium supplemented with $(NH_4)_2SO_4$ for 2 d and treated as independent biological replicates. The cells were washed with deionized water and subcultured in N-free medium for two more days. On the day of the experiment, the cultures were washed three times with deionized water and inoculated in N-free medium at an initial OD_{600} of 0.05. The cultures were grown at 28°C at 185 rpm, and OD_{600} was measured at different time points, as indicated in the graph. The experiment was conducted for 72 h. For each strain and each time point, three to six OD_{600} values were taken for every biological replicate. Mean ± SE was calculated for individual time points for every strain.

$\delta^{15}N$ Stable Isotope Analyses in Rice Shoots

Rice plants were treated with MS (control) or JGTA-S1. The treatments were repeated at 3 wpi, and the plants were grown for one more week. The shoot tissues were separated and dried as described above. Dried shoot tissue from 10 plants was pooled to obtain 1 g each of the biological replicate.

The stable isotope analyses were performed at the Archeology Department, University of Cape Town, with six such replicates per treatment. Values were expressed relative to the standard for atmospheric N for $\delta^{15}N$, as (%), according to the following equation:

$$\delta Z = \left(R_{\text{sample}}/R_{\text{standard}} - 1\right) \times 1000$$

where Z is the heavy isotope of N, and R is the ratio of heavier to lighter isotope for the sample and standard ($^{15}N/^{14}N$). The oven-dried plant components were milled and the combusted in a Flash 2000 organic elemental analyzer. Three different in-house standards (Merck Gel, lentil [*Lens culinaris*], and *Acacia saligna*) were used and calibrated against the standards of the International Atomic Energy Agency. N is expressed relative to atmospheric N.

Estimation of P Levels in Plant Tissues

Plant samples were oven dried (60°C for 48 h) and pulverized. Each 100-mg plant sample was digested with 2.5 mL of concentrated HNO_3 (65% [v/v], Merck) and 2.5 mL of H_2O_2 (30% [v/v], Merck). The digested samples were filtered through Whatman 110-nm filter paper followed by a 0.22-μm filter. The total P in the digest was measured by inductively coupled plasma optical emission spectroscopy (iCAP duo 6500, Thermo Fisher Scientific; radio frequency power, 1150 W; pump rate, 50 rpm; auxiliary gas flow, 1 L/min; nebulizer gas flow, 0.6 L/min; and coolant gas flow, 12 L/min). National Institute of Standards and Technology River Sediment Sample Standard Reference Material 1645 digested in the same manner as the experimental samples was used as a standard.

Transmission Electron Microscopy of Yeast Cells

Prefixative solution (2× 0.4 M Pipes, pH 6.8, 0.4 M sorbitol, 4 mM $MgCl_2$, 4 mM $CaCl_2$, 8% [v/v] glutaraldehyde, and water to 20 mL) was added to a JGTA-S1 culture ($OD_{600} = 0.6$) at a 1:1 (v/v) ratio, followed by incubation for 5 min at room temperature. The cells were centrifuged at 1500*g* for 5 min at room temperature. The supernatant was discarded, and the cells were suspended in 1× prefixative and incubated overnight at 4°C. The cells were washed three times with 1× prefixative without glutaraldehyde at 4°C and resuspended in 50 mM Tris-HCl, pH 7.5, 5 mM $MgCl_2$, 1.4 M sorbitol, and 0.5% (v/v) 2-mercaptoethanol plus 0.15 mg/mL zymolyase for 10 min at room temperature. The cells were washed with 1× prefixative without glutaraldehyde and fixed in 0.5% (w/v) osmium tetroxide and 0.8% (w/v) potassium ferrocyanide (Bauer et al., 2001) in distilled water two times for 5 min each time at 4°C. The cells were washed five to six times with 1× prefixative without glutaraldehyde, stored at 4°C, sectioned, and viewed under a microscope.

Statistical Analysis

All graphing and statistical analyses were performed using Prism 7.0 (GraphPad Software). Normality of variables was evaluated by D'Agostino-Pearson Omnibus test. The growth-promoting effects of JGTA-S1 treatment on rice (increases in total dry mass, root and shoot length, chlorophyll content, P content per plant, and total N content per plant) were analyzed using Mann-Whitney unpaired two-tailed *t* test. Statistical analysis of the RT-qPCR data was performed using unpaired *t* test. Nitrate contents in JGTA-S1–, 11.3-, 11.3+Ps-, and JGTA-R3–treated plants were statistically analyzed by one-way ANOVA followed by Tukey's post hoc test. Ammonium content and biomass of JGTA-S1–, 11.3-, 11.3+Ps-, and JGTA-R3–treated plants were statistically analyzed by Kruskal-Wallis nonparametric test followed by Dunn's post correction test. Acetylene reduction data were also analyzed using Kruskal-Wallis nonparametric test followed by Dunn's post correction test and Mann-Whitney U-test. The values were plotted in box plots. Dunn's multiple comparisons were performed to compare groups. Normally distributed two-sample groups were compared by Student's unpaired *t* test. For $\delta^{15}N$ stable isotope analysis, the values were statistically analyzed by Student's *t* test. For the growth curve, mean ± SE was calculated per individual time point for every strain. A value of P value < 0.05 was considered statistically significant. Bars with different letters indicate significant differences among groups. All data are given as mean ± SE. A summary of the test statistics is provided in Supplemental Data Set 1.

Supplemental Data

Supplemental Figure 1. *Rhodotorula mucilaginosa* JGTA-S1 promotes the growth of rice varieties IR64 and Bordan.

Supplemental Figure 2. Cluster analysis of the expression levels of DEGs in shoots and roots using Multiple Experiment Viewer with Pearson Correlation.

Supplemental Figure 3. Validation of the microarray data with selected genes.

Supplemental Figure 4. Total phosphate levels in rice do not significantly change in response to JGTA-S1 inoculation.

Supplemental Figure 5. *R. mucilaginosa* JGTA-S1 improves N metabolism in rice irrespective of rice variety.

Supplemental Figure 6. JGTA-S1 forms chains when grown in the absence of N.

Supplemental Figure 7. JGTA-S1 contains endobacteria, some of which are diazotrophs.

Supplemental Figure 8. Removal of bacteria reduces JGTA-S1 fitness in N-free medium.

Supplemental Data Set 1. Summary of statistical tests.

Supplemental Data Set 2. Differentially regulated rice shoot transcripts at 24 hpi with JGTA-S1.

Supplemental Data Set 3. Differentially regulated rice root transcripts at 24 hpi with JGTA-S1.

Supplemental Data Set 4. Major DEGs in rice regulated upon JGTA-S1 treatment.

Supplemental Data Set 5. Comparison of data with Coneva et al. 2014 (GSE61370): Normal versus induced N and 24 hpi JGTA-S1 treated versus control root data.

Supplemental Data Set 6. Comparison with Obertello et al. 2015 (GSE38102): +N versus –N and 24 hpi JGTA-S1 treated versus control root data.

Supplemental Data Set 7. List of primers used in this study.

ACKNOWLEDGMENTS

We thank Maitrayee Dasgupta, Department of Biochemistry, Calcutta University, for the LIVE DEAD bacterial stain. We thank Madhumanti Das for her help in the characterization of JGTA-S1. We also thank the Department of Biotechnology-Interdisciplinary Programme of Life Sciences for advanced Research and Education [DBT-IPLS], Calcutta University, for the use of the confocal microscopy facility and Arijit Pal and Souvik Roy for their technical assistance in microscopy. Funding was provided by the Department of Biotechnology, Ministry of Science and Technology (Project BT/PR15410/BCE/08/861/2011) and by Calcutta University (University Grants Commission-University with Potential for Excellence [UGC-UPE] to K.P.).

AUTHOR CONTRIBUTIONS

C.S. and K.P. performed most of the experiments, helped in preparing the article, and prepared the figures. C.S. prepared the graphs in GraphPad Prism. All figures were created by K.P. M.N. performed some of the JGTA-S1 and JGTA-R3 interaction analysis, M.N. and G.M. participated in nitrate measurements; H.N. participated in the spotting assay; D.M., S.S., S.M., and M.P.S. performed the acetylene reduction assays; D.S. and S.Tripathy performed JGTA-S1 genome analysis and OrthoMCL study; N.N. and S.L. measured P; S. Tripathi helped measure total N; and D.B. helped with some RT-PCR studies. M.K. and M.B. performed transmission electron microscopy of JGTA-S1. A.K. and A.J.V. performed the N_2-isotope analysis. U.D.G. helped with sample collection and initial analysis of JGTA-S1. A.S. designed the experiments, created the strains, and wrote the article.

Received June 4, 2019; revised October 25, 2019; accepted November 19, 2019; published November 22, 2019.

REFERENCES

Abaidoo, R.C., Keyser, H.H., Singleton, P.W., and Borthakur, D. (2002). Comparison of molecular and antibiotic resistance profile methods for the population analysis of *Bradyrhizobium* spp. (TGx) isolates that nodulate the new TGx soybean cultivars in Africa. J. Appl. Microbiol. **92:** 109–117.

Akhtyamova, N., and Sattarova, R.K. (2013). Endophytic yeast *Rhodotorula rubra* strain TG-1: Antagonistic and plant protection activities. Biochem. Physiol. **2:** 104.

Arnon, D.I. (1949). Copper enzymes in isolated chloroplasts. Polyphenoloxidase in *Beta vulgaris*. Plant Physiol. **24:** 1–15.

Barbieri, E., Bertini, L., Rossi, I., Ceccaroli, P., Saltarelli, R., Guidi, C., Zambonelli, A., and Stocchi, V. (2005). New evidence for bacterial diversity in the ascoma of the ectomycorrhizal fungus *Tuber borchii* Vittad. FEMS Microbiol. Lett. **247:** 23–35.

Barbieri, E., Guidi, C., Bertaux, J., Frey-Klett, P., Garbaye, J., Ceccaroli, P., Saltarelli, R., Zambonelli, A., and Stocchi, V. (2007). Occurrence and diversity of bacterial communities in *Tuber magnatum* during truffle maturation. Environ. Microbiol. **9:** 2234–2246.

Barzanti, R., Ozino, F., Bazzicalupo, M., Gabbrielli, R., Galardi, F., Gonnelli, C., and Mengoni, A. (2007). Isolation and characterization of endophytic bacteria from the nickel hyperaccumulator plant *Alyssum bertolonii*. Microb. Ecol. **53:** 306–316.

Bauer, C., Herzog, V., and Bauer, M.F. (2001). Improved technique for electron microscope visualization of yeast membrane structure. Microsc. Microanal. **7:** 530–534.

Benedito, V.A., et al. (2008). A gene expression atlas of the model legume *Medicago truncatula*. Plant J. **55:** 504–513.

Bi, Y.-M., et al. (2009). Increased nitrogen-use efficiency in transgenic rice plants over-expressing a nitrogen-responsive early nodulin gene identified from rice expression profiling. Plant Cell Environ. **32:** 1749–1760.

Bolano, A., Stinchi, S., Preziosi, R., Bistoni, F., Allegrucci, M., Baldelli, F., Martini, A., and Cardinali, G. (2001). Rapid methods to extract DNA and RNA from *Cryptococcus neoformans*. FEMS Yeast Res. **1:** 221–224.

Brown, M.E., and Metcalfe, G. (1957). Nitrogen fixation by a species of *Pullularia*. Nature **180:** 282.

Bulgarelli, D., et al. (2012). Revealing structure and assembly cues for Arabidopsis root-inhabiting bacterial microbiota. Nature **488:** 91–95.

Cao, L.X., You, J.L., and Zhou, S.N. (2002). Endophytic fungi from *Musa acuminata* leaves and roots in South China. World J. Microbiol. Biotechnol. **18:** 169–171.

Carvalho, T.L., Balsemão-Pires, E., Saraiva, R.M., Ferreira, P.C., and Hemerly, A.S. (2014). Nitrogen signalling in plant interactions with associative and endophytic diazotrophic bacteria. J. Exp. Bot. **65:** 5631–5642.

Cataldo, D.A., Maroon, M., Schrader, L.E., and Youngs, V.L. (1975). Rapid colorimetric determination of nitrate in plant tissue by nitration of salicylic acid. Commun. Soil Sci. Plant Anal. **6:** 71–80.

Chevalier, D., Batoux, M., Fulton, L., Pfister, K., Yadav, R.K., Schellenberg, M., and Schneitz, K. (2005). STRUBBELIG defines a receptor kinase-mediated signaling pathway regulating organ development in Arabidopsis. Proc. Natl. Acad. Sci. USA **102:** 9074–9079.

Coneva, V., Simopoulos, C., Casaretto, J.A., El-Kereamy, A., Guevara, D.R., Cohn, J., Zhu, T., Guo, L., Alexander, D.C., Bi, Y.M., McNicholas, P.D., and Rothstein, S.J. (2014). Metabolic and co-expression network-based analyses associated with nitrate response in rice. BMC Genomics **15:** 1056.

Dobbelaere, S., Vanderleyden, J., and Okon, Y. (2003). Plant growth-promoting effects of diazotrophs in the rhizosphere. Crit. Rev. Plant Sci. **22:** 107–149.

Du, Z., Zhou, X., Ling, Y., Zhang, Z., and Su, Z. (2010). agriGO: A GO analysis toolkit for the agricultural community. Nucleic Acids Res. **38:** W64–W70.

Edwards, J., Johnson, C., Santos-Medellín, C., Lurie, E., Podishetty, N.K., Bhatnagar, S., Eisen, J.A., and Sundaresan, V. (2015). Structure, variation, and assembly of the root-associated microbiomes of rice. Proc. Natl. Acad. Sci. USA **112:** E911–E920.

Estrada-De Los Santos, P., Bustillos-Cristales, R., and Caballero-Mellado, J. (2001). *Burkholderia*, a genus rich in plant-associated nitrogen fixers with wide environmental and geographic distribution. Appl. Environ. Microbiol. **67:** 2790–2798.

Ferris, P.J., and Goodenough, U.W. (1997). Mating type in *Chlamydomonas* is specified by mid, the minus-dominance gene. Genetics **146:** 859–869.

Figueiredo, A., Monteiro, F., and Sebastiana, M. (2014). Subtilisin-like proteases in plant-pathogen recognition and immune priming: A perspective. Front. Plant Sci. **5:** 739.

Firrincieli, A., Otillar, R., Salamov, A., Schmutz, J., Khan, Z., Redman, R.S., Fleck, N.D., Lindquist, E., Grigoriev, I.V., and Doty, S.L. (2015). Genome sequence of the plant growth promoting endophytic yeast *Rhodotorula graminis* WP1. Front. Microbiol. **6:** 978.

Fisher, R.M., Henry, L.M., Cornwallis, C.K., Kiers, E.T., and West, S.A. (2017). The evolution of host-symbiont dependence. Nat. Commun. **8:** 15973.

Gai, C.S., Lacava, P.T., Maccheroni, W., Jr., Glienke, C., Araújo, W.L., Miller, T.A., and Azevedo, J.L. (2009). Diversity of endophytic yeasts from sweet orange and their localization by scanning electron microscopy. J. Basic Microbiol. **49:** 441–451.

Gancedo, J.M. (2001). Control of pseudohyphae formation in *Saccharomyces cerevisiae*. FEMS Microbiol. Rev. **25:** 107–123.

Gauthier, G.M. (2015). Dimorphism in fungal pathogens of mammals, plants, and insects. PLoS Pathog. **11:** e1004608.

Gehrig, H., Schüssler, A., and Kluge, M. (1996). *Geosiphon pyriforme*, a fungus forming endocytobiosis with *Nostoc* (cyanobacteria), is an ancestral member of the Glomales: Evidence by SSU rRNA analysis. J. Mol. Evol. **43:** 71–81.

Geurts, R., Xiao, T.T., and Reinhold-Hurek, B. (2016). What does it take to evolve a nitrogen-fixing endosymbiosis? Trends Plant Sci. **21:** 199–208.

Gutiérrez, R.A., Stokes, T.L., Thum, K., Xu, X., Obertello, M., Katari, M.S., Tanurdzic, M., Dean, A., Nero, D.C., McClung, C.R., and Coruzzi, G.M. (2008). Systems approach identifies an organic nitrogen-responsive gene network that is regulated by the master clock control gene CCA1. Proc. Natl. Acad. Sci. USA **105:** 4939–4944.

Gutjahr, C., Sawers, R.J., Marti, G., Andrés-Hernández, L., Yang, S.Y., Casieri, L., Angliker, H., Oakeley, E.J., Wolfender, J.L., Abreu-Goodger, C., and Paszkowski, U. (2015). Transcriptome diversity among rice root types during asymbiosis and interaction with arbuscular mycorrhizal fungi. Proc. Natl. Acad. Sci. USA **112:** 6754–6759.

Hiruma, K., Gerlach, N., Sacristán, S., Nakano, R.T., Hacquard, S., Kracher, B., Neumann, U., Ramírez, D., Bucher, M., O'Connell, R.J., and Schulze-Lefert, P. (2016). Root endophyte *Colletotrichum tofieldiae* confers plant fitness benefits that are phosphate status dependent. Cell **165:** 464–474.

Hogan, D.A., and Kolter, R. (2002). *Pseudomonas-Candida* interactions: An ecological role for virulence factors. Science **296:** 2229–2232.

Horst, R.J., Zeh, C., Saur, A., Sonnewald, S., Sonnewald, U., and Voll, L.M. (2012). The *Ustilago maydis* Nit2 homolog regulates nitrogen utilization and is required for efficient induction of filamentous growth. Eukaryot. Cell **11:** 368–380.

Khan, Z., Guelich, G., Phan, H., Redman, R., and Doty, S. (2012). Bacterial and yeast endophytes from poplar and willow promote growth in crop plants and grasses. ISRN Agron. **2012:** 1–11.

Kneip, C., Lockhart, P., Voss, C., and Maier, U.G. (2007). Nitrogen fixation in eukaryotes--New models for symbiosis. BMC Evol. Biol. **7:** 1–12.

Knoth, J.L., Kim, S.-H., Ettl, G.J., and Doty, S.L. (2013). Effects of cross host species inoculation of nitrogen-fixing endophytes on growth and leaf physiology of maize. Glob. Change Biol. Bioenergy **5:** 408–418.

Knoth, J.L., Kim, S.-H., Ettl, G.J., and Doty, S.L. (2014). Biological nitrogen fixation and biomass accumulation within poplar clones as a result of inoculations with diazotrophic endophyte consortia. New Phytol. **201:** 599–609.

Kobayashi, D.Y., and Crouch, J.A. (2009). Bacterial/fungal interactions: From pathogens to mutualistic endosymbionts. Annu. Rev. Phytopathol. **47:** 63–82.

Konishi, M., and Yanagisawa, S. (2013). Arabidopsis NIN-like transcription factors have a central role in nitrate signalling. Nat. Commun. **4:** 1617.

Koroleff, F. (1976). Determination of ammonia. In Methods of Seawater Analysis, K. Grasshoft, ed (Weinheim: Verlag Chemie), pp. 126–133.

Larran, S., Mónaco, C., and Alippi, H.E. (2001). Endophytic fungi in leaves of *Lycopersicon esculentum* Mill. World J. Microbiol. Biotechnol. **17:** 181–184.

Larran, S., Perelló, A., Simón, M.R., and Moreno, V. (2002). Isolation and analysis of endophytic microorganisms in wheat (*Triticum aestivum* L.) leaves. World J. Microbiol. Biotechnol. **18:** 683–686.

Lee, S.C., Li, A., Calo, S., and Heitman, J. (2013). Calcineurin plays key roles in the dimorphic transition and virulence of the human pathogenic zygomycete *Mucor circinelloides*. PLoS Pathog. **9:** e1003625.

Leroy, C., Jauneau, A., Martinez, Y., Cabin-Flaman, A., Gibouin, D., Orivel, J., and Séjalon-Delmas, N. (2017). Exploring fungus-plant N transfer in a tripartite ant-plant-fungus mutualism. Ann. Bot. **120:** 417–426.

Li, L., Stoeckert, C.J., Jr., and Roos, D.S. (2003). OrthoMCL: Identification of ortholog groups for eukaryotic genomes. Genome Res. **13:** 2178–2189.

Li, R., Zhang, H., Liu, W., and Zheng, X. (2011). Biocontrol of postharvest gray and blue mold decay of apples with *Rhodotorula mucilaginosa* and possible mechanisms of action. Int. J. Food Microbiol. **146:** 151–156.

Liu, Y.G., Mitsukawa, N., Oosumi, T., and Whittier, R.F. (1995). Efficient isolation and mapping of *Arabidopsis thaliana* T-DNA insert junctions by thermal asymmetric interlaced PCR. Plant J. **8:** 457–463.

Lundberg, D.S., et al. (2012). Defining the core *Arabidopsis thaliana* root microbiome. Nature **488:** 86–90.

MacDonald, R.M., and Chandler, M.R. (1981). Bacterium-like organelles in the vesicular-arbuscular mycorrhizal fungus *Glomus caledonius*. New Phytol. **89:** 241–246.

Márquez, L.M., Redman, R.S., Rodriguez, R.J., and Roossinck, M.J. (2007). A virus in a fungus in a plant: three-way symbiosis required for thermal tolerance. Science **315:** 513–515.

Martínez-Espinoza, A.D., León, C., Elizarraraz, G., and Ruiz-Herrera, J. (1997). Monomorphic nonpathogenic mutants of *Ustilago maydis*. Phytopathology **87:** 259–265.

Minerdi, D., Fani, R., Gallo, R., Boarino, A., and Bonfante, P. (2001). Nitrogen fixation genes in an endosymbiotic *Burkholderia* strain. Appl. Environ. Microbiol. **67:** 725–732.

Moebius, N., Üzüm, Z., Dijksterhuis, J., Lackner, G., and Hertweck, C. (2014). Active invasion of bacteria into living fungal cells. eLife **3:** e03007.

Nassar, A., El-Tarabily, K., and Sivasithamparam, K. (2005). Promotion of plant growth by an auxin-producing isolate of the yeast *Williopsis saturnus* endophytic in maize (*Zea mays* L.) roots. Biol. Fertil. Soils **42:** 97–108.

Nogueira, E.M., Vinagre, F., Masuda, H.P., Vargas, C., Pádua, V.L.M., Silva, F.R., Santos, R.V., Baldani, J.I., Ferreira, P.C.G., and Hemerly, A.S. (2001). Expression of sugarcane genes induced by inoculation with *Gluconacetobacter diazotrophicus* and *Herbaspirillum rubrisubalbicans*. Genet. Mol. Biol. **24:** 199–206.

Obertello, M., Shrivastava, S., Katari, M.S., and Coruzzi, G.M. (2015). Cross-species network analysis uncovers conserved nitrogen-regulated network modules in rice. Plant Physiol. **168:** 1830–1843.

Partida-Martinez, L.P., and Hertweck, C. (2005). Pathogenic fungus harbours endosymbiotic bacteria for toxin production. Nature **437:** 884–888.

Partida-Martinez, L.P., Monajembashi, S., Greulich, K.O., and Hertweck, C. (2007). Endosymbiont-dependent host reproduction maintains bacterial-fungal mutualism. Curr. Biol. **17:** 773–777.

Pearce, G., Yamaguchi, Y., Barona, G., and Ryan, C.A. (2010). A subtilisin-like protein from soybean contains an embedded, cryptic signal that activates defense-related genes. Proc. Natl. Acad. Sci. USA **107:** 14921–14925.

Peiffer, J.A., Spor, A., Koren, O., Jin, Z., Tringe, S.G., Dangl, J.L., Buckler, E.S., and Ley, R.E. (2013). Diversity and heritability of the maize rhizosphere microbiome under field conditions. Proc. Natl. Acad. Sci. USA **110:** 6548–6553.

Pinto-Tomás, A.A., Anderson, M.A., Suen, G., Stevenson, D.M., Chu, F.S.T., Cleland, W.W., Weimer, P.J., and Currie, C.R. (2009). Symbiotic nitrogen fixation in the fungus gardens of leaf-cutter ants. Science **326:** 1120–1123.

Ramakers, C., Ruijter, J.M., Deprez, R.H., and Moorman, A.F. (2003). Assumption-free analysis of quantitative real-time polymerase chain reaction (PCR) data. Neurosci. Lett. **339:** 62–66.

Reid, D.E., Ferguson, B.J., Hayashi, S., Lin, Y.H., and Gresshoff, P.M. (2011). Molecular mechanisms controlling legume autoregulation of nodulation. Ann. Bot. **108:** 789–795.

Rogers, C., and Oldroyd, G.E. (2014). Synthetic biology approaches to engineering the nitrogen symbiosis in cereals. J. Exp. Bot. **65:** 1939–1946.

Ruiz-Herrera, J., León-Ramírez, C., Vera-Nuñez, A., Sánchez-Arreguín, A., Ruiz-Medrano, R., Salgado-Lugo, H., Sánchez-Segura, L., and Peña-Cabriales, J.J. (2015). A novel intracellular nitrogen-fixing symbiosis made by *Ustilago maydis* and *Bacillus* spp. New Phytol. **207:** 769–777.

Saha, C., and Seal, A. (2015). Early changes in shoot transcriptome of rice in response to *Rhodotorula mucilaginosa* JGTA-S1. Genom. Data **6:** 237–240.

Saha, C., Mukherjee, G., Agarwal-Banka, P., and Seal, A. (2016). A consortium of non-rhizobial endophytic microbes from *Typha angustifolia* functions as probiotic in rice and improves nitrogen metabolism. Plant Biol. (Stuttg.) **18:** 938–946.

Sampedro, I., Aranda, E., Scervino, J.M., Fracchia, S., García-Romera, I., Ocampo, J.A., and Godeas, A. (2004). Improvement by soil yeasts of arbuscular mycorrhizal symbiosis of soybean (*Glycine max*) colonized by *Glomus mosseae*. Mycorrhiza **14:** 229–234.

Sánchez-Martínez, C., and Pérez-Martín, J. (2001). Dimorphism in fungal pathogens: *Candida albicans* and *Ustilago maydis*--Similar inputs, different outputs. Curr. Opin. Microbiol. **4:** 214–221.

Scannerini, S., and Bonfante, P. (1991). Bacteria and bacteria like objects in endomycorrhizal fungi (Glomaceae). In Symbiosis as Source of Evolutionary Innovation: Speciation and Morphogenesis, L. Margulis, and and R. Fester, eds (Cambridge: MIT Press), pp. 273–287.

Schlaeppi, K., Dombrowski, N., Oter, R.G., Ver Loren van Themaat, E., and Schulze-Lefert, P. (2014). Quantitative divergence of the bacterial root microbiota in *Arabidopsis thaliana* relatives. Proc. Natl. Acad. Sci. USA **111:** 585–592.

Sen, D., Paul, K., Saha, C., Mukherjee, G., Nag, M., Ghosh, S., Das, A., Seal, A., and Tripathy, S. (2019). A unique life-strategy of an endophytic yeast *Rhodotorula mucilaginosa* JGTA-S1-A comparative genomics viewpoint. DNA Res. **26:** 131–146.

Sharma, M., Schmid, M., Rothballer, M., Hause, G., Zuccaro, A., Imani, J., Kämpfer, P., Domann, E., Schäfer, P., Hartmann, A., and Kogel, K.H. (2008). Detection and identification of bacteria intimately associated with fungi of the order Sebacinales. Cell. Microbiol. **10:** 2235–2246.

Soltis, D.E., Soltis, P.S., Morgan, D.R., Swensen, S.M., Mullin, B.C., Dowd, J.M., and Martin, P.G. (1995). Chloroplast gene sequence data suggest a single origin of the predisposition for symbiotic nitrogen fixation in angiosperms. Proc. Natl. Acad. Sci. USA **92:** 2647–2651.

Staehelin, C., Xie, Z.-P., Illana, A., and Vierheilig, H. (2011). Long-distance transport of signals during symbiosis: Are nodule formation and mycorrhization autoregulated in a similar way? Plant Signal. Behav. **6:** 372–377.

Steward, G.F., Zehr, J.P., Jellison, R., Montoya, J.P., and Hollibaugh, J.T. (2004). Vertical distribution of nitrogen-fixing

phylotypes in a meromictic, hypersaline lake. Microb. Ecol. **47:** 30–40.

Tian, X.L., Cao, L.X., Tan, H.M., Zeng, Q.G., Jia, Y.Y., Han, W.Q., and Zhou, S.N. (2004). Study on the communities of endophytic fungi and endophytic actinomycetes from rice and their antipathogenic activities in vitro. World J. Microbiol. Biotechnol. **20:** 303–309.

Torres-Cortés, G., Ghignone, S., Bonfante, P., and Schüßler, A. (2015). Mosaic genome of endobacteria in arbuscular mycorrhizal fungi: Transkingdom gene transfer in an ancient mycoplasma-fungus association. Proc. Natl. Acad. Sci. USA **112:** 7785–7790.

Trdá, L., Fernandez, O., Boutrot, F., Héloir, M.C., Kelloniemi, J., Daire, X., Adrian, M., Clément, C., Zipfel, C., Dorey, S., and Poinssot, B. (2014). The grapevine flagellin receptor VvFLS2 differentially recognizes flagellin-derived epitopes from the endophytic growth-promoting bacterium Burkholderia phytofirmans and plant pathogenic bacteria. New Phytol. **201:** 1371–1384.

Valdivia, R.H., and Heitman, J. (2007). Endosymbiosis: The evil within. Curr. Biol. **17:** R408–R410.

Vandenkoornhuyse, P., Quaiser, A., Duhamel, M., Le Van, A., and Dufresne, A. (2015). The importance of the microbiome of the plant holobiont. New Phytol. **206:** 1196–1206.

Vinagre, F., Vargas, C., Schwarcz, K., Cavalcante, J., Nogueira, E.M., Baldani, J.I., Ferreira, P.C., and Hemerly, A.S. (2006). SHR5: A novel plant receptor kinase involved in plant-N2-fixing endophytic bacteria association. J. Exp. Bot. **57:** 559–569.

Wang, R., Dong, L., Chen, Y., Qu, L., Wang, Q., and Zhang, Y. (2017). *Esteya vermicola*, a nematophagous fungus attacking the pine wood nematode, harbors a bacterial endosymbiont affiliated with Gammaproteobacteria. Microbes Environ. **32:** 201–209.

Xin, G., Glawe, D., and Doty, S.L. (2009). Characterization of three endophytic, indole-3-acetic acid-producing yeasts occurring in *Populus* trees. Mycol. Res. **113:** 973–980.

Yan, D., et al. (2016). NIN-like protein 8 is a master regulator of nitrate-promoted seed germination in Arabidopsis. Nat. Commun. **7:** 13179.

Ye, J., Coulouris, G., Zaretskaya, I., Cutcutache, I., Rozen, S., and Madden, T.L. (2012). Primer-BLAST: A tool to design target-specific primers for polymerase chain reaction. BMC Bioinformatics **13:** 134.

Zhang, H., Ge, L., Chen, K., Zhao, L., and Zhang, X. (2014). Enhanced biocontrol activity of *Rhodotorula mucilaginosa* cultured in media containing chitosan against postharvest diseases in strawberries: Possible mechanisms underlying the effect. J. Agric. Food Chem. **62:** 4214–4224.

Zimmer, B.L., and Roberts, G.D. (1979). Rapid selective urease test for presumptive identification of *Cryptococcus neoformans*. J. Clin. Microbiol. **10:** 380–381.